Physics 7450: Solid State Physics 2

Lecture 5: Electron liquid

Leo Radzihovsky

(Dated: 10 March, 2015)

Abstract

In these lectures, we will study itinerate electron liquid, namely metals. We will begin by reviewing properties of noninteracting electron gas, developing its Greens functions, analyzing its thermodynamics, Pauli paramagnetism and Landau diamagnetism. We will recall how its thermodynamics is qualitatively distinct from that of a Boltzmann and Bose gases. As emphasized by Sommerfeld (1928), these qualitative difference are due to the Pauli principle of electons' fermionic statistics. We will then include effects of Coulomb interaction, treating it in Hartree and Hartree-Fock approximation, computing the ground state energy and screening. We will then study itinerate Stoner ferromagnetism as well as various response functions, such as compressibility and conductivity, and screening (Thomas-Fermi, Debye). We will then discuss Landau Fermi-liquid theory, which will allow us understand why despite strong electron-electron interactions, nevertheless much of the phenomenology of a Fermi gas extends to a Fermi liquid. We will conclude with discussion of electrons on the lattice, treated within the Hubbard and t-J models and will study transition to a Mott insulator and magnetism

I. INTRODUCTION

A. Outline

- electron gas ground state and excitations
- thermodynamics
- Pauli paramagnetism
- Landau diamagnetism
- Hartree-Fock theory of interactions: ground state energy
- Stoner ferromagnetic instability
- response functions
- Landau Fermi-liquid theory
- electrons on the lattice: Hubbard and t-J models
- Mott insulators and magnetism

B. Background

In these lectures, we will study itinerate electron liquid, namely metals. In principle a fully quantum mechanical, strongly Coulomb-interacting description is required. However, as discovered by Sommerfeld (1928) and put on a more solid footing by Landau (1957)[1], it is truly amazing that much of conventional metals's phenomenology can be captured by weakly interacting (even noninteracting) Fermi gas, with Pauli exclusion principle being the key crucial ingredient that distinguishes the system the Boltzmann and Bose gases.

Of course for a more refined description, to capture the distinction between metals (partially filled band) and band-insulators (fully filled band) a crystalline lattice potential must be incorporated. It leads to spectra of bands separated by band-gaps with the wealth of phenomenology on which semiconductors are based. To understand the existence of non-interacting the so-called Anderson insulators, where a band is only partially filled, as first emphasized by P. W. Anderson electron transport in the presence of lattice imperfections (random potential) must be included. Furthermore, to understand the existence electron liquid's instabilities to charge- and spin-density wave (where charge or spin crystalize into a periodically modulated state), superconducting, (the so-called) Mott insulating[5], ferromagnetic states electron-electron interactions must be crucially taken into account. Although this is quite challenging and cannot be done exactly, a variety of physically inspired (numerics, perturbation theory, Hartree and Hartree-Fock) approximations allow one to make significant progress.

We will therefore begin by reviewing properties of noninteracting electron gas, studying its ground state and excitations, developing its Greens functions, analyzing its thermodynamics, Pauli paramagnetism and Landau diamagnetism. We will then include effects of Coulomb interaction, treating it in Hartree and Hartree-Fock approximation, computing the ground state energy and screening. We will then study itinerate Stoner ferromagnetism as well as various response functions, such as compressibility, conductivity, Thomas-Fermi screening and the general electromagnetic response. We will conclude with discussion of electrons on the lattice, treated within the Hubbard and t-J models and will study transition to a Mott insulator and magnetism, thereby making contact with lecture set 4 on magnetic insulators.

II. NONINTERACTING FERMI GAS

A. Ground state

As discussed in the Introduction, much of the phenomenology of simple metals can be captured by ideal Fermi gas, described by a noninteracting Hamiltonian $H_0 = -\sum_{i=1}^{N} \frac{\hbar^2}{2m}\nabla_i^2$, that in the second-quantized form is given by

$$\begin{aligned} H_0 &= \int d^d r \psi_\sigma^\dagger \left(\frac{-\hbar^2\nabla^2}{2m}\right) \psi_\sigma^\dagger, && (1) \\ &= \sum_{\mathbf{k},\sigma=\uparrow,\downarrow} \epsilon_k c_{\mathbf{k},\sigma}^\dagger c_{\mathbf{k},\sigma}, && (2) \end{aligned}$$

where the Pauli exclusion principle is automatically incorporated through the anticommutation relation of fermionic creation and annihilation field operators, $\{\psi_\sigma(\mathbf{r}), \psi_{\sigma'}^\dagger(\mathbf{r}')\} = \delta_{\sigma,\sigma'}\delta^d(\mathbf{r}-\mathbf{r}')$, $\{\psi_\sigma(\mathbf{r}), \psi_{\sigma'}(\mathbf{r}')\} = 0$, $\{\psi_\sigma^\dagger(\mathbf{r}), \psi_{\sigma'}^\dagger(\mathbf{r}')\} = 0$, and their Fourier transform operators, $c_{\mathbf{k},\sigma}, c_{\mathbf{k},\sigma}^\dagger$, where $\sigma \in \uparrow, \downarrow$ is the spin coordinate, the dispersion $\epsilon_k = \frac{\hbar^2 k^2}{2m}$ is the kinetic energy at momentum $\hbar\mathbf{k}$.

The first-quantized N-electron eigenstate is given by an antisymmetrized product (Slater determinant)

$$\Psi_{\alpha,\beta,\ldots}(\mathbf{r}_1,\sigma_1,\mathbf{r}_2,\sigma_2,\ldots,\mathbf{r}_N,\sigma_N) = \frac{1}{\sqrt{N}}\sum_P(-1)^{n_P}\psi_\alpha(\mathbf{r}_{P(1)},\sigma_{P(1)})\psi_\alpha(\mathbf{r}_{P(2)},\sigma_{P(2)})\ldots, \quad (3)$$

$$= \langle\mathbf{r}_1,\sigma_1,\mathbf{r}_2,\sigma_2,\ldots,\mathbf{r}_N,\sigma_N|c^\dagger_\alpha c^\dagger_\beta c^\dagger_\gamma\ldots|0\rangle, \quad (4)$$

of single-electron eigenstates $\psi_\alpha(\mathbf{r},\sigma)$, that are plane-waves (with $\alpha=\mathbf{k}=\frac{2\pi}{L}(n_x,n_y,n_z)$) in the absence of an external single-particle potential. It is convenient to utilize the second-quantized occupation basis form,

$$|\{n_{\mathbf{k},\sigma}\}\rangle = \prod_{\mathbf{k},\sigma}\left[(c^\dagger_{\mathbf{k},\sigma})^{n_{\mathbf{k},\sigma}}\right]|0\rangle, \quad (5)$$

with occupation numbers $n_{\mathbf{k},\sigma}\in 0,1$ eigenvalues of the occupation number operator $\hat{n}_{\mathbf{k},\sigma} = c^\dagger_{\mathbf{k},\sigma}c_{\mathbf{k},\sigma}$.

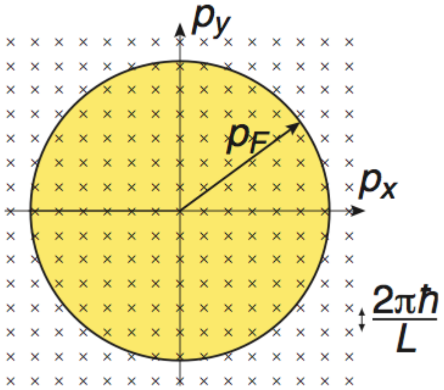

FIG. 1: Ground state of a 2d Fermi gas, with all states with $k<k_F$ filled by two $\uparrow,\downarrow$ electrons (yellow) and empty for $k>k_F$.

The electron gas ground state (see Fig.1) is then given by occupation of states with the lowest single-particle energies $\epsilon_{\mathbf{k}}$, with 2 electrons $\sigma=\uparrow,\downarrow$ per state, that we denote as Fermi sea, $|FS\rangle$. For a system with isotropic dispersion, this corresponds to

$$n_{\mathbf{k}} = \begin{cases} 1, \text{ for } |\mathbf{k}|<k_F, \\ 0, \text{ for } |\mathbf{k}|\geq k_F, \end{cases}, \quad (6)$$

where total number of atoms N is related to the highest occupied Fermi momentum state

k_F and Fermi energy $\epsilon_F = \frac{\hbar^2 k_F}{2m}$,

$$\begin{aligned} N &= \sum_{\mathbf{k},\sigma} 1 = 2\sum_{\mathbf{k}} 1 = 2L^d \int_0^{k_F} \frac{d^d k}{(2\pi)^d} 1 \equiv 2L^d \int \frac{d^d k}{(2\pi)^d} n_{\mathbf{k}}, && (7)\\ &\equiv \int_0^{\epsilon_F} d\epsilon g(\epsilon), && (8)\\ &= 2L^d C_d k_F^d/d. && (9) \end{aligned}$$

Above $C_d \equiv S_d/(2\pi)^d$ and $S_d = 2\pi^{d/2}/\Gamma(d/2)$ is the surface area of a $d-1$ dimensional unit sphere, $S_1 = 2, S_2 = 2\pi, S_3 = 4\pi$ and $g(\epsilon) = C_d \left(\frac{2m}{\hbar^2}\right)^{d/2} \epsilon^{d/2-1} =_{3d} \frac{1}{2\pi^2}\left(\frac{2m}{\hbar^2}\right)^{3/2} \epsilon^{1/2} = \frac{3}{2} n(\epsilon)/\epsilon$ is the density of states. Consistent with dimensional analysis, above expresses the density n in terms of the Fermi momentum and Fermi energy, $n \sim k_F^d \sim \epsilon_F^{d/2}$, with 3d case $n_{3d} = \frac{k_F^3}{3\pi^2}$. The total ground state energy is then given by

$$\begin{aligned} E_{FS} &= \sum_{\mathbf{k},\sigma} \frac{\hbar^2 k^2}{2m} = 2\sum_{\mathbf{k}} \epsilon_{\mathbf{k}} n_{\mathbf{k}} = 2L^d \int_0^{k_F} \frac{d^d k}{(2\pi)^d} \frac{\hbar^2 k^2}{2m} = \int_0^{\epsilon_F} d\epsilon \epsilon g(\epsilon), && (10)\\ &= 2C_d \frac{\hbar^2 k_F^2}{2m} \frac{k_F^d L^d}{d+2} = \frac{d}{d+2} N\epsilon_F =_{d=3} \frac{3}{5} N\epsilon_F. && (11) \end{aligned}$$

The pressure is also straightforward to calculate, at $T = 0$ given by

$$\begin{aligned} P &= -\frac{\partial E}{\partial V}|_N = -N\frac{d}{d+2}\frac{\partial \epsilon_F}{\partial V}|_N, && (12)\\ &= \frac{2}{d+2} n\epsilon_F =_{d=3} \frac{2}{5} n\epsilon_F., && (13) \end{aligned}$$

where we used the homogeneity property of $\epsilon_F \propto V^{-2/d}$ and introduced density $n = N/V$. We note that this expression is of the ideal gas law form ($PV = Nk_B T$) with $T_F = \epsilon_F/k_B$ playing the role of T at zero temperature. Above relations also give a relation $E = \frac{3}{2}PV$, that is a generic consequence of quadratic spectrum and extends to finite temperature.

Thus for metals, where there is an electron per ion separated by a few angstroms, Pauli principle leads to anormous kinetic energies, pressure and velocities even at $T = 0$, with $k_F \sim 1/$, $\epsilon_F \sim eV \sim 10^4$ Kelvin, $v_F \sim 10^6$ m/sec. Thus, electrons in a metal even at room temperature are highly "degenerate" with $k_B T_{room}/\epsilon_F \ll 1$. Of course, because in a time-reversal symmetric case ($B = 0$), $\pm\mathbf{k}, \pm\sigma$ are equally occupied, the net momentum and magnetization vanishes in the ground state.

B. Excitations

1. *single-particle electron-hole excitations*

The excited states of the Fermi gas consists of many-body states, where one of the electrons is excited to higher single-particle energy states. Since electrons are conserved, excited electrons come from the Fermi sea, leaving a hole in its place. Relative to the ground state $|FS\rangle$ such electron and hole carry positive energy, latter because it corresponds to a missing electron below ϵ_F. It is convenient to work in the grand-canonical formulation,

$$H_0 \rightarrow H_\mu = H_0 - \mu N = \sum_{\mathbf{k},\sigma=\uparrow,\downarrow} \varepsilon_k c^\dagger_{\mathbf{k},\sigma} c_{\mathbf{k},\sigma},$$

where single particle energy $\varepsilon_{\mathbf{k}} = \epsilon_k - \mu$ is now measured relative to the chemical potential that at zero temperature is given by Fermi energy, $\mu = \epsilon_F$.

More formally we can introduce new operators for electron ($k > k_F$) and hole ($k < k_F$) excitations,

$$d_{\mathbf{k}\sigma} = \begin{cases} c^\dagger_{\mathbf{k},\sigma}, & \text{for } |\mathbf{k}| > k_F, \\ c_{\mathbf{k},\sigma}, & \text{for } |\mathbf{k}| < k_F, \end{cases} , \tag{14}$$

with Fermi sea as its Pauli principle imposed vacuum, namely

$$d_{\mathbf{k}\sigma}|FS\rangle = 0.$$

In terms of these the Hamiltonian separates into the ground state Fermi sea energy E_{FS} and explicitely positive excitations

$$\begin{aligned} H_0 &= \sum_{k<k_F,\sigma} \varepsilon_k d_{\mathbf{k}\sigma} d^\dagger_{\mathbf{k}\sigma} + \sum_{k>k_F,\sigma} \varepsilon_k d^\dagger_{\mathbf{k}\sigma} d_{\mathbf{k}\sigma}, & (15)\\ &= E_{FS} + \sum_{k<k_F,\sigma} (\epsilon_F - \epsilon_k) d^\dagger_{\mathbf{k}\sigma} d_{\mathbf{k}\sigma} + \sum_{k>k_F,\sigma} (\epsilon_k - \epsilon_F) d^\dagger_{\mathbf{k}\sigma} d_{\mathbf{k}\sigma}, & (16)\\ &= E_{FS} + \sum_{\mathbf{k},\sigma} |\epsilon_k - \epsilon_F| d^\dagger_{\mathbf{k}\sigma} d_{\mathbf{k}\sigma} = E_{FS} + \sum_{\mathbf{k},\sigma} |\varepsilon_k| d^\dagger_{\mathbf{k}\sigma} d_{\mathbf{k}\sigma}, & (17) \end{aligned}$$

with the positive excitation energy $|\varepsilon_k|$ illustrated in Fig.(2) Similarly for momentum

$$\begin{aligned} \mathbf{P} &= \sum_{\mathbf{k},\sigma} \hbar \mathbf{k} c^\dagger_{\mathbf{k}\sigma} c_{\mathbf{k}\sigma}, & (18)\\ &= \sum_{k<k_F,\sigma} (-\hbar \mathbf{k}) d^\dagger_{\mathbf{k}\sigma} d_{\mathbf{k}\sigma} + \sum_{k>k_F,\sigma} \hbar \mathbf{k} d^\dagger_{\mathbf{k}\sigma} d_{\mathbf{k}\sigma}, & (19) \end{aligned}$$

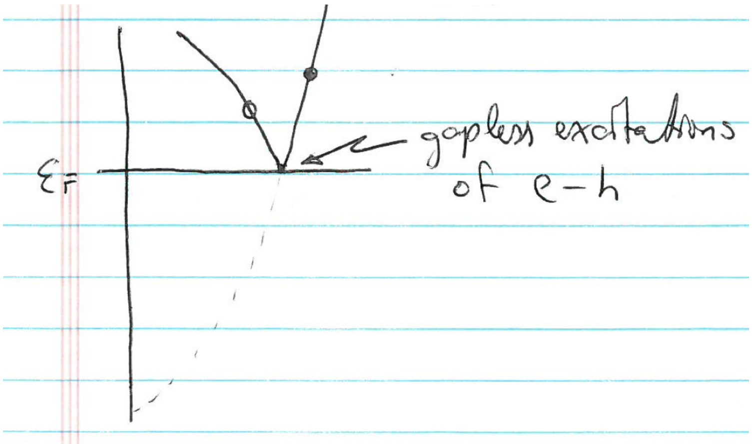

FIG. 2: Electron and hole positive energy excitation in the Fermi sea ground state.

we see that hole carries negative momentum $-\hbar\mathbf{k}$.

Since electrons are conserved, the simplest excitation is an electron-hole pair $c^\dagger_{\mathbf{k}+\mathbf{q}\sigma}c_{\mathbf{q}\sigma}$ (sum over spin σ implied and will be suppressed), where an electron with momentum $\mathbf{q}$ inside FS is promoted to a state $\mathbf{q}+\mathbf{k}$, corresponding to an excited state $|\mathbf{k},\mathbf{q}\rangle = c^\dagger_{\mathbf{k}+\mathbf{q}}c_{\mathbf{q}}|FS\rangle$ with net momentum of the pair $\mathbf{k}$. We note that a superposition of such electron-hole pairs over the relative momentum $\mathbf{q}$ corresponds to a density excitation at momentum $\mathbf{k}$

$$\rho(\mathbf{k}) = \int_{\mathbf{r}} \psi^\dagger(\mathbf{r})\psi(\mathbf{r})e^{-i\mathbf{k}\cdot\mathbf{r}} = \sum_{\mathbf{q}} c^\dagger_{\mathbf{k}+\mathbf{q}}c_{\mathbf{q}}. \tag{20}$$

The excitation energy $E^{eh}_{\mathbf{k},\mathbf{q}}$ is a function of both the center of mass ($\mathbf{k}$) and the relative ($\mathbf{q}$) momenta

$$E_{\mathbf{k},\mathbf{q}} = \left(\frac{\hbar^2(\mathbf{k}+\mathbf{q})^2}{2m} - \epsilon_F\right) + \left(\epsilon_F - \frac{\hbar^2\mathbf{q}^2}{2m}\right), \tag{21}$$

$$= \frac{\hbar^2\mathbf{k}^2}{2m} + \frac{\hbar^2\mathbf{k}\cdot\mathbf{q}}{m}, \tag{22}$$

bounded by $E^{eh}_{min}(\mathbf{k}) \leq E^{eh}_{\mathbf{k},\mathbf{q}} \leq E^{eh}_{max}(\mathbf{k})$, where

$$E^{eh}_{min,max}(\mathbf{k}) = \frac{\hbar^2k^2}{2m} \mp \frac{\hbar^2 k q_F}{m},$$

illustrated in Fig.(3).

The presence of continuum can be understood by considering the nature of e-h excitations defining the boundaries $E^{eh}_{max}(\mathbf{k}), E^{eh}_{min}(\mathbf{k})$. The upper boundary $E^{eh}_{max}(\mathbf{k})$ is defined by the center of mass momentum $\mathbf{k}$, starting at 0 and increasing along $\mathbf{q}_F$, as illustrated in Fig.(4)

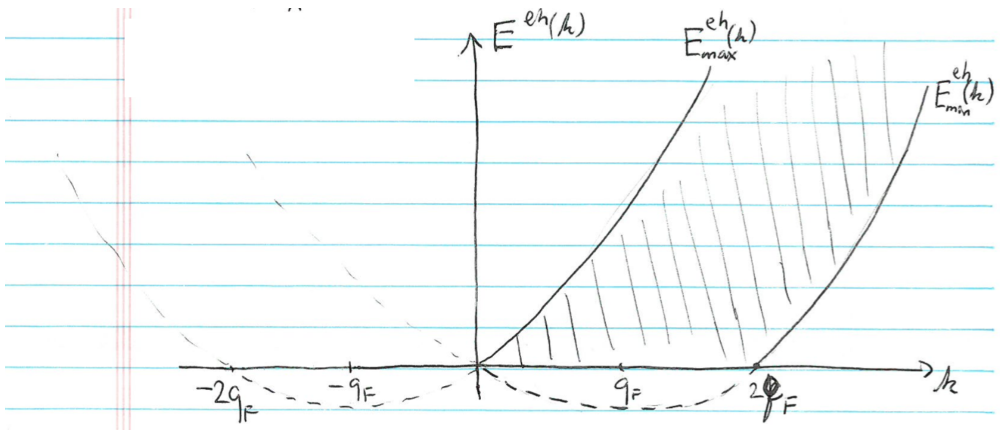

FIG. 3: Two-particle electron-hole spectral continuum, $E^{eh}_{\mathbf{k},\mathbf{q}}$.

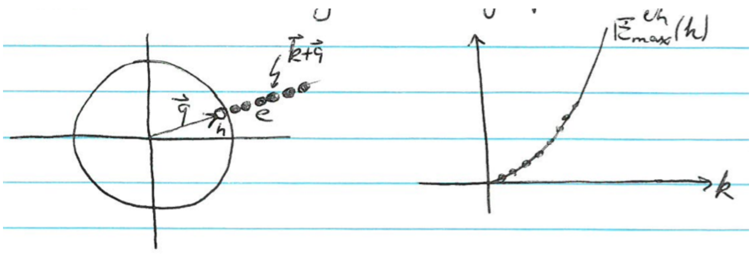

FIG. 4: Upper boundary, $E^{eh}_{max}(\mathbf{k})$ of the two-particle electron-hole continuum, corresponding to $\mathbf{k}$ increasing along $\mathbf{q}_F$.

The lower boundary $E^{eh}_{min}(\mathbf{k})$ is defined by the center of mass momentum $\mathbf{k}$, starting at $-2\mathbf{q}_F$ across the Fermi sea, and increasing along $-\mathbf{q}_F$, as illustrated in Fig.(5) The zero energy boundary $E^{eh}(\mathbf{k}, \mathbf{q}) = 0$ is defined by the center of mass momentum $\mathbf{k}$, starting at 0 and increasing toward $-2\mathbf{q}_F$ along the boundary of the Fermi surface, as illustrated in Fig.(6)

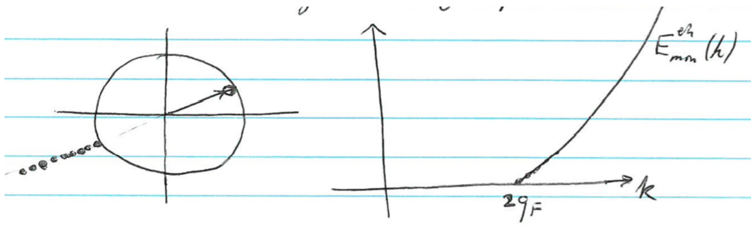

FIG. 5: Lower boundary, $E^{eh}_{min}(\mathbf{k})$ of the two-particle electron-hole continuum, corresponding to $\mathbf{k}$ increasing along $-\mathbf{q}_F$.

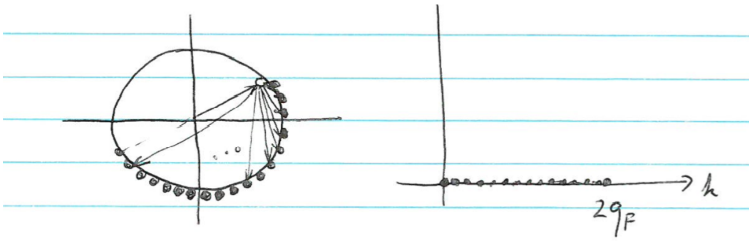

FIG. 6: Zero energy boundary, $E^{eh}(\mathbf{k},\mathbf{q}) = 0$ of the two-particle electron-hole continuum, corresponding to $\mathbf{k}$ starting at 0 and increasing toward $-2\mathbf{q}_F$ along the boundary of the Fermi surface.

2. collective charge density plasmon excitations

In addition to above electron-hole excitations, in the presence of Coulomb interactions there are collective plasmon excitations. We will derive this result in a more microscopic way when include role of interactions in the microscopic electron Hamiltonian. However, here we will derive the collective mode from a more general hydrodynamic theory,

$$\partial_t\rho + \boldsymbol{\nabla}\cdot\mathbf{g} = 0, \tag{23}$$

$$\partial_t\mathbf{g} = en\mathbf{E} - \kappa^{-1}\boldsymbol{\nabla}\rho, \tag{24}$$

where $\rho = mn$, $\mathbf{g} = mn\mathbf{v}$ are mass and momentum density, respectively, satisfying the mass continuity equation, (23) and Newton's momentum balance equation, (24), $\mathbf{E}$ is the electric field induced by charge fluctuation and κ is mass compressibility.

Within a linear approximation $n \approx n_0$ of a constant background density inside the electric field term, taking the time derivative of the first and divergence of the second equations allows us to eliminate $\mathbf{g}$ using Gauss's law, $\boldsymbol{\nabla}\cdot\mathbf{E} = 4\pi e\rho/m$, obtaining

$$\partial_t^2\rho + \frac{4\pi n e^2}{m}\rho - \kappa^{-1}\nabla^2\rho \;=\; 0, \tag{25}$$

$$\tag{26}$$

which leads to collective *gapped* plasmon mode with quadratic dispersion

$$\omega_p(k) = \sqrt{\omega_{p0}^2 + c_p^2 k^2}, \tag{27}$$

with plasma frequency

$$\omega_p = \sqrt{\frac{4\pi n e^2}{m}},$$

that joins the electron-hole continuum as illustrated in Fig.(7)

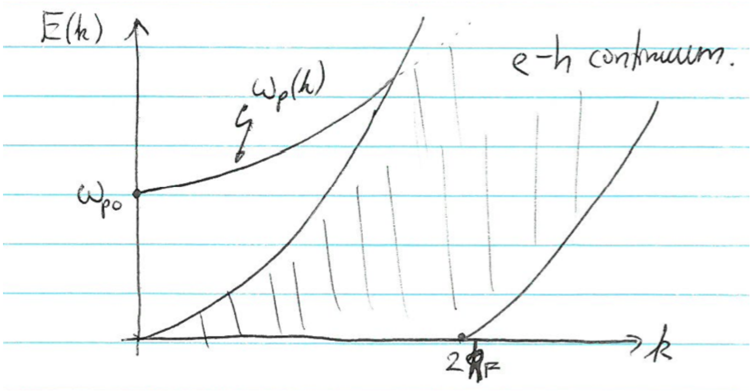

FIG. 7: Plasmon mode decaying into the electron-hole continuum.

C. Thermodynamics

The thermodynamics is conveniently computed in the grand-canonical ensemble, encoded by the partition function

$$Z_{gr} = \mathrm{Tr} e^{-\beta(\hat{H}-\mu\hat{N})} = \sum_{\{n_{\mathbf{k}\sigma}\}} e^{-\beta\sum_{\mathbf{k}\sigma}(\epsilon_k-\mu)n_{\mathbf{k}\sigma}}, \tag{28}$$

$$= \prod_{\mathbf{k}\sigma}\left(\sum_{n_{\mathbf{k}\sigma}} e^{-\beta(\epsilon_k-\mu)n_{\mathbf{k}\sigma}}\right), \tag{29}$$

$$= \prod_{\mathbf{k}\sigma}\left(1+e^{-\beta(\epsilon_k-\mu)}\right), \tag{30}$$

which gives the grand-canonical free energy

$$\Pi_{gr} = -k_BT\ln Z_{gr} = -k_BT\sum_{\mathbf{k}\sigma}\ln\left(1+e^{-\beta(\epsilon_k-\mu)}\right), \tag{31}$$

$$= -k_BTL^d\int d\epsilon g(\epsilon)\ln\left(1+e^{-\beta(\epsilon-\mu)}\right), \tag{32}$$

and also the pressure through $PV = -\Pi_{gr}$. With this, we can also calculate the total number of particles (or equivalently density n) as a function of chemical potential and temperature

$$N = -\frac{\partial\Pi_{gr}}{\partial\mu} = \sum_{\mathbf{k},\sigma}\frac{1}{e^{\beta(\epsilon_k-\mu)}+1} \equiv \sum_{\mathbf{k},\sigma}\langle n_{\mathbf{k}\sigma}\rangle, \tag{33}$$

where the average occupation function is the Fermi-Dirac distribution,

$$\langle n_{\mathbf{k}\sigma}\rangle = \frac{1}{e^{\beta(\epsilon_k-\mu)}+1} \equiv f(\epsilon_k) \approx \begin{cases} e^{-\beta(\epsilon_k-\mu)}, & \text{for } \mu \ll k_BT, \text{ nondegenerate,} \\ \theta(\mu-\epsilon_k), & \text{for } \mu \gg k_BT, \text{ degenerate,} \end{cases}$$

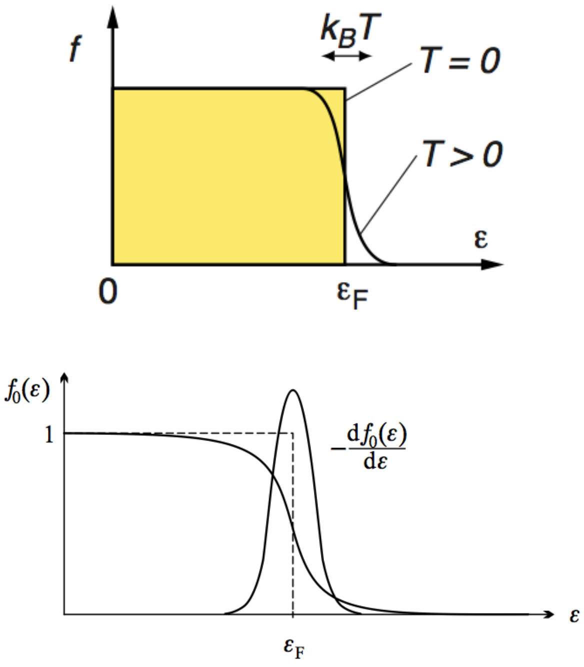

FIG. 8: Fermi-Dirac distribution describing finite T momentum states occupation in the noninteracting Fermi gas and the corresponding derivative.

illustrated below The average occupation $\langle n_{\mathbf{k}\sigma}\rangle$ can also be computed more directly via

$$\langle \hat{n}_{\mathbf{k}\sigma}\rangle = \frac{1}{Z_{gr}} \mathrm{Tr}\left(\hat{n}_{\mathbf{k}\sigma} e^{-\beta \hat{H}}\right).$$

Using $f(\epsilon_k)$ and the density of states to perform the sum in the thermodynamic limit, we obtain

$$N = V\int_0^\infty d\epsilon g(\epsilon) f(\epsilon), \tag{34}$$

$$= \frac{V}{2\pi^2}\left(\frac{2m}{\hbar^2}\right)^{3/2}\int_0^\infty d\epsilon \epsilon^{1/2} f(\epsilon) = 2V\left(\frac{mk_BT}{2\pi\hbar^2}\right)^{3/2} F_{1/2}(\mu/k_BT), \tag{35}$$

where

$$F_{1/2}(x) = \frac{2}{\sqrt{\pi}}\int_0^\infty \frac{\epsilon^{1/2} d\epsilon}{e^{\epsilon - x}+1}$$

is the order 1/2 Fermi integral that can be evaluated numerically. Using $F_j(x \to -\infty) \to e^x$, in the classical limit of $e^{\mu/k_BT} \ll 1$, we recover the classical Boltzmann gas result $n = 2\left(\frac{mk_BT}{2\pi\hbar^2}\right)^{3/2} e^{\mu/k_BT}$, giving $\mu \approx -k_BT\ln[1/(n\lambda_T^3)] \sim -T\ln T$ (λ_T is thermal deBroglie wavelength, that in the classical limit is much smaller than interparticle spacing).

In the opposite limit $\mu/k_BT \gg 1$ relevant to metals, we utilize large x expansion, $F_{1/2}(x) \approx \frac{4}{3\sqrt{\pi}} x^{3/2}\left(1+\frac{\pi^2}{8x^2}+\ldots\right)$, obtaining

$$n = \frac{1}{3\pi^2}\left(\frac{2m\mu}{\hbar^2}\right)^{3/2}\left(1+\frac{\pi^2}{8}\left(\frac{k_BT}{\mu}\right)^2+\ldots\right),$$

that by definition of the Fermi energy (derived in sections above) is also given by $n = \frac{1}{3\pi^2}\left(\frac{2m\epsilon_F}{\hbar^2}\right)^{3/2}$, consistent with $\mu(T=0)=\epsilon_F$ and giving

$$\mu = \epsilon_F\left[1-\frac{\pi^2}{12}\left(\frac{k_BT}{\epsilon_F}\right)^2\ldots\right].$$

We can understand this weak reduction of μ with increasing T by noting (see Fig.(8)) that for fixed μ the area under the curve (including the $\epsilon^{1/2}$ density of states factor) *increases* with T broading: although to lowest order the decrease from rounding below μ is compensated by a tail above μ, low ϵ is cutoff at $\epsilon = 0$, while high ϵ tail extends to infinity. Thus to keep the electron number fixed at N, the chemical potential, $\mu(T)$ must *decrease* with increasing T to compensate this excited electron-hole imbalance.

The energy and heat capacity are also straightforwardly computed either directly or through the derivative of the free-energy, giving

$$E = 2\sum_{\mathbf{k}}\epsilon_k f(\epsilon_k), \tag{36}$$

$$C_{el} = \frac{\partial E}{\partial T}, \tag{37}$$

for $T=0$ reducing to results obtained in previous subsection. We leave a detailed evaluation of these as a homework exercise, only quoting the 3d $T\to 0$ limit result

$$c_{el} \equiv C_{el}/V = \frac{\pi^2}{3}g(\epsilon_F)k_B^2T \equiv \gamma T,$$

where γ is referred to as the Sommerfeld coefficient. The full result is illustrated in Fig.(9), interpolates betweent the high temperature classical equipartition result of $\frac{1}{2}dNk_B$ and the low-T result above. In interacting systems γ is substantially different form above free electron gas, with the difference attributed to the effective mass increase due to interactions. This general linear T dependence, that is hallmark of simple metals (a truimph of the Sommerfeld theory) is a direct consequence of the Pauli principle. Namely, at low T only a small fraction $k_BT/\epsilon_F \ll 1$ of the Fermi sea close to the Fermi surface can participate in excitations, others

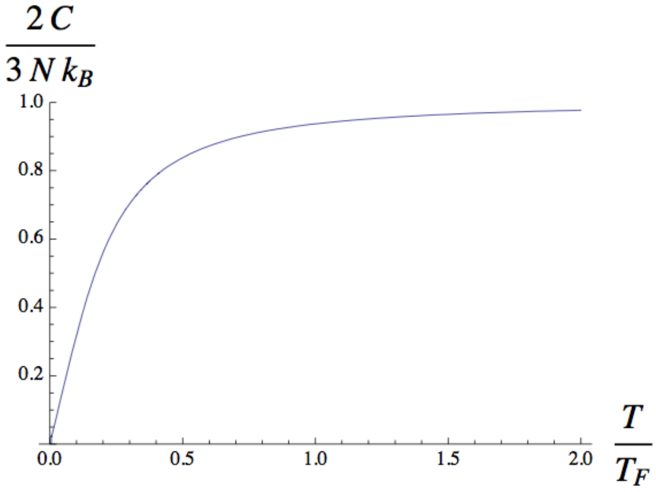

FIG. 9: Electronic heat capacity $C_{el}(T)$, interpolating betweent the high temperature classical equipartition result of $\frac{1}{2}dNk_B$ and the low-T result γT one.[6]

are Pauli blocked. This small fraction of electrons then equipartitions the thermal energy, thereby giving

$$E_{excitation} \approx N\left(\frac{k_BT}{\epsilon_F}\right)k_BT,$$

whose derivative immediately leads to the linear T dependence (rather than the constant classical Nk_B result) of simple metals, quoted above.

A systemmatic general analysis of the low-temperature behavior of any electronic quantities can be obtained using the so-called Sommerfeld expansion, which relies on the sharpness of the derivative of the Fermi-Dirac distribution function at low T. Namely, integrating by parts to bring out the sharp feature of the FD distribution at low T, for a generic average we obtain

$$\langle H\rangle = \int_{-\infty}^{\infty} d\epsilon H(\epsilon)f(\epsilon), \tag{38}$$

$$= \int_{-\infty}^{\infty} d\epsilon\left(\int_{-\infty}^{\mu+(\epsilon-\mu)} H(\epsilon')d\epsilon'\right)\frac{\partial f}{\partial\mu}, \tag{39}$$

which can then Taylor expanded in $\epsilon-\mu \approx O[(k_BT/\epsilon_F)^2]$.

Having established the basics of the noninteracting Fermi gas, we next turn to its response to an external magnetic field for Fermi gas (still ignoring interactions).

D. Pauli paramagnetism

As we have seen above, the ground state of a noninteracting Fermi gas is nonmagnetic, with spin up and down states equally populated. On general grounds we therefore expect that in the presence of an external magnetic field these spin states will be split by the eigenvalues of the Zeeman

$$H_Z = -\boldsymbol{\mu}\cdot\mathbf{B} = \frac{g\mu_B}{\hbar}\mathbf{S}\cdot\mathbf{B} = \mu_B B\sigma_z,$$

$\epsilon_{\uparrow,\downarrow} = \pm\mu_B B$. Ignoring orbital effects of the magnetic field (that we will consider in the next subsection), together with the kinetic energy the single-electron spectrum is then given by

$$\epsilon_{\mathbf{k}\sigma} = \frac{\hbar^2 k^2}{2m} + \sigma\mu_B B, \quad \sigma = \pm 1.$$

As before we determine the chemical potential $\mu(n, T, B)$ through the constraint on the total electron number density $n = N/V$

$$\begin{aligned} n &= n_\downarrow + n_\uparrow = V^{-1}\sum_{\mathbf{k}} f(\epsilon_{\mathbf{k}\downarrow}) + V^{-1}\sum_{\mathbf{k}} f(\epsilon_{\mathbf{k}\uparrow}), && (40)\\ &= \int_{-\mu_B B}^{\infty} d\epsilon g(\epsilon+\mu_B B) f(\epsilon) + \int_{\mu_B B}^{\infty} d\epsilon g(\epsilon-\mu_B B) f(\epsilon), && (41)\\ & && (42)\end{aligned}$$

The spin magnetization response (in the absence of orbital effects) is simply the difference between $n_\uparrow, n_\downarrow$ densities

$$\begin{aligned} m &= \mu_B \int_{-\mu_B B}^{\infty} d\epsilon g(\epsilon+\mu_B B) f(\epsilon) - \mu_B \int_{\mu_B B}^{\infty} d\epsilon g(\epsilon-\mu_B B) f(\epsilon), && (43)\\ &= \mu_B \int_0^{\infty} d\epsilon g(\epsilon)\left[f(\epsilon-\mu_B B) - f(\epsilon+\mu_B B)\right], && (44)\\ &\approx \mu_B^2 B \int_0^{\infty} d\epsilon g(\epsilon)\frac{-\partial f(\epsilon)}{\partial\epsilon} = \mu_B^2 g(\epsilon_F) B, \quad \text{for } \mu_B B \ll \epsilon_F, \quad T\to 0, && (45)\end{aligned}$$

where the last expression is evaluated in the weak B linear response, $T = 0$ limit, utilizing δ-function form of the derivative of the Fermi-Dirac distribution.

Above coupled integrals can be computed numerically, giving the full expression for $m(n, T, B)$ after using $\mu(n, T, B)$ from the number equation. At $T = 0$, the full magnetization can be straightforwardly calculated analytically using $f_{T=0}(x) = \theta(\epsilon_F - x)$,

$$m = \mu_B \left[\int_{-\mu_B B}^{\epsilon_F} d\epsilon g(\epsilon + \mu_B B) - \int_{\mu_B B}^{\epsilon_F} d\epsilon g(\epsilon - \mu_B B) \right], \tag{46}$$

$$= \mu_B c_d \int_{\epsilon_F - \mu_B B}^{\epsilon_F + \mu_B B} d\epsilon\, \epsilon^{d/2-1} = \mu_B c_d \frac{2}{d} \left[(\epsilon_F + \mu_B B)^{d/2} - (\epsilon_F - \mu_B B)^{d/2} \right], \tag{47}$$

$$\approx \chi_{Pauli} B, \quad \text{for } B \to 0 \tag{48}$$

where density of states $g(\epsilon) = c_d \epsilon^{d/2-1}$ was used with overall constants packaged into c_d, finding Pauli linear susceptibility

$$\chi_{Pauli} = \frac{d}{2} \frac{n\mu_B^2}{\epsilon_F} = \mu_B^2 g(\epsilon_F), \tag{49}$$

to be compared to the Curie susceptibility $\chi_{Curie} \sim \frac{\mu_B^2}{k_B T}$, with the role of $k_B T$ replaced by ϵ_F. As with the qualitative discussion of the low-temperature excitation energy and the heat capacity, above, here too we can understand the result of the temperature-independent Pauli susceptibility in terms of Curie susceptibility of the reduced, temperature dependent number of excitations confined by the Pauli principle to the $k_B T/\epsilon_F$ shell around the Fermi surface. This reproduces the detailed result via

$$\chi_{Pauli} \sim \frac{k_B T}{\epsilon_F} \chi_{Curie} = \frac{k_B T}{\epsilon_F} \frac{\mu_B^2}{k_B T} = \frac{\mu_B^2}{\epsilon_F}.$$

The Wilson ratio (K.G. Wilson, 1975) for a free electron gas is therefore given by

$$R_W \equiv \frac{\chi_P}{c_{el}} = \frac{3}{\pi^2 T} \left(\frac{\mu_B}{k_B} \right)^2.$$

A substantial deviation (e.g., even a factor of 2) of R_W from above ideal value is usually attributed to strong electron-electron correlations.

Above we have focussed on magnetic response to an external field due to spins, ignoring orbital effects of charged electrons.

E. Landau diamagnetism

In addition to the Zeeman spin effect, $H_{Zeeman} = \frac{g\mu_B}{\hbar} \mathbf{S} \cdot \mathbf{B}$ of an external magnetic field analyzed above, electrons are charged particles and so respond to orbital effects of the magnetic field by executing Larmor orbits, resulting in circulating currents that contribute to magnetization m. According to the ...theorem discussed in lecture notes ..., within purely

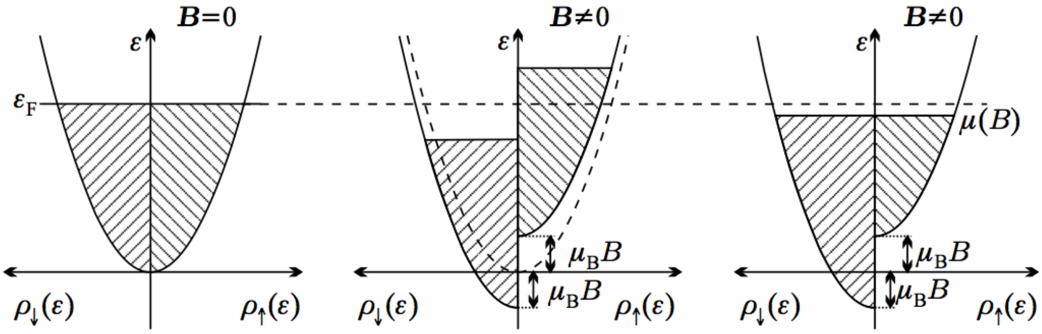

FIG. 10: The electronic density of states for the two spin orientations, in the absence a magnetic field (left) and in its presence, before spin-flip and spin-transfer equilibration processes take place (middle) and in thermal equilibrium (right).[6]

classical treatment there is no orbital magnetism. However, within a quantum treatment, indeed orbital response to a magnetic field is diamagnetic with the (so-called) Landau susceptibility for free electrons is given by

$$\chi_{Landau} = -\frac{1}{3}\chi_{Pauli}, \tag{50}$$

i.e., exactly 1/3 of the Pauli paramagnetic susceptibility. Qualitatively, the diamagnetic response can be thought of as a reflection of Lenz law, where in response to an externally applied B field electrons produce orbital currents that reduce the associated induced of flux.

We now turn to a detailed derivation of the above seminal result and related ones. Since we have already treated Pauli spin contribution, for simplcity we will neglect spin, by for example imagining it to be fully polarized by the external magnetic field. To study the orbital effects of the magnetic field, we need to first solve the Schrodinger equation of an electron ina magnetic field, a problem first solve by L.D. Landau (1930),

$$\frac{1}{2m}\left(-i\hbar\boldsymbol{\nabla} + e\mathbf{A}\right)^2 \psi(\mathbf{r}) = E\psi(\mathbf{r}),$$

where the electromagnetic vector potential corresponds to the background constant magnetic field $\boldsymbol{\nabla} \times \mathbf{A} = \mathbf{B}$. The two most convenient convenient and commonly used gauge forms of the vector potential are: (i) Landau gauge, $\mathbf{A} = (0, Bx, 0)$ and (ii) symmetric gauge, $\mathbf{A} = \frac{1}{2}\mathbf{B} \times \mathbf{r} = \frac{1}{2}B(-y, x, 0)$. This is a standard quantum mechanics problem, that we will not reproduce here referring the reader to an excellent and detailed exposition in Solyom Solids II[6] and elsewhere, instead simply quoting the results that we need for studying Landau's orbital magnetism and later the quantum Hall effect.

Following Landau, working in the gauge named after him, we observe that the Hamiltonian is translationally invariant along y and z, with eigenstates therefore plane-waves in the yz plane. In the x variable the Hamiltonian is that of a harmonic oscillator centered around k_y dependent minimum. We thus find in 3d, that the spectrum and eigenstates are given by

$$\psi_{n,k_y,k_z}(x,y,z) = N_n H_n\left(\frac{x-x_{k_y}}{\ell}\right) e^{-(x-x_{k_y})^2/2\ell^2} e^{ik_y y+ik_z z}, \tag{51}$$

$$E_{n,k_y,k_z}(x,y,z) = \hbar\omega_c(n+\frac{1}{2})+\frac{\hbar^2 k_z^2}{2m}, \tag{52}$$

where $\omega_c = eB/m$ is the cyclotron frequency, $\ell = \sqrt{\frac{\hbar}{m\omega_c}} = \sqrt{\frac{\phi_0}{2\pi B}}$ is the magnetic length, setting the scale of the extent of the wavefunctions in the x direction, the size of the cyclotron orbit of its semiclassical trajectory, $x_{k_y} = \ell^2 k_y$ is the center of the Gaussian state labelled by k_y, , $N_n = (\pi^{1/2}\ell 2^n n!)^{-1/2}$ is the normalization. Quantum number n labels the Landau levels, that because of translational invariance in x exhibit macroscopic degeneracy with respect to $k_y = x_{k_y}/\ell^2$, physically associated with degeneracy with respect to the location x_{k_y} of the orbitals within the sample of width L_x,

$$g_n = \frac{L_x L_y}{2\pi\ell^2} = \frac{BA}{\phi_0},$$

and equals to the total number of flux quanta piercing the sample area A.

We note that magnetic field quenches xy-plane kinetic energy perpendicular to $\mathbf{B}$, but leaves the dispersion along it noninteracting k_z^2. We also observe that including spin the dispersion becomes (taking $g \approx 2$)

$$\begin{aligned} E_{\sigma,n,k_y,k_z}(x,y,z) &= \hbar\omega_c(n+\frac{1}{2})+\frac{\hbar^2 k_z^2}{2m}+\frac{1}{2}g\mu_B B\sigma, &(53)\\ &= \hbar\omega_c\left[n+\frac{1}{2}(1+\sigma)\right]+\frac{\hbar^2 k_z^2}{2m} &(54)\end{aligned}$$

with each Landau level split for $\sigma = \pm 1$ by $\hbar\omega_c$, leading to a zero $E_{-1,n=0,k_z=0} = 0$ mode. Moving on we will again ignore spin as its effects can be accounted for by a factor of 2 in all but the zeroth Landau level.

Now that we computed the spectrum we can calculate the orbital response to the external magnetic field by standard thermodynamic calculations. These are simplified when expressed in terms of the density of states, $g(B,\epsilon)$. In 2d the density of states is a comb of δ-functions of strength g_n (degeneracy of each level)

$$g_{2d}(\epsilon) = A^{-1}\sum_n g_n \delta[\epsilon - \hbar\omega_c(n+1/2)] \approx \frac{g_n}{\hbar\omega_c} = \frac{B}{\phi_0\hbar\omega_c} = \frac{m}{2\pi\hbar^2},$$

where the second equality comes after coarse-graining on energy scale large compared to $\hbar\omega_c$, such that n can be treated as a continuous variable (replacing the sum by an integral), giving g_n levels per $\hbar\omega_c$ energy interval. As illustrated in Fig.(11) states in the nth Landau level arise from collapse of the $B = 0$ states for $n\hbar\omega_c < \epsilon < (n+1)\hbar\omega_c$

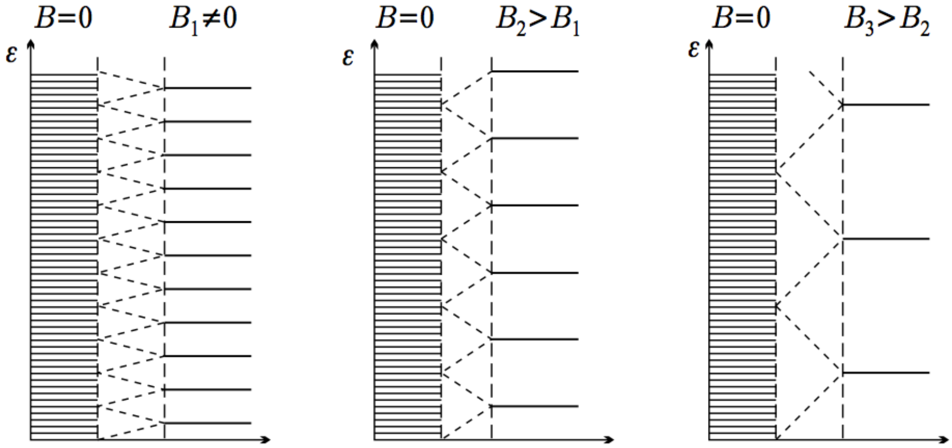

FIG. 11: Collapse of continuous $B = 0$ spectrum into Landau levels at finite magnetic field.[6]

Turning now to the 3d case, we have an additional k_z quantum number quantized in units of $L_z/2\pi$. Per each Landau level n we have $dN_n = g_n \frac{L_z}{2\pi} dk_z$ states in the interval dk_z. Using $k_z(\epsilon)$, including a factor of 2 for spin and summing Landau levels, we obtain

$$g_{3d}(\epsilon, B) = \sum_{n,k_z,\sigma} g_n \delta\left(\epsilon - (n+\frac{1}{2})\hbar\omega_c - \frac{\hbar^2 k_z^2}{2m}\right), \tag{55}$$

$$= 2L_z \sum_n \int \frac{dk_z}{2\pi} g_n \delta\left(\epsilon - (n+\frac{1}{2})\hbar\omega_c - \frac{\hbar^2 k_z^2}{2m}\right), \tag{56}$$

$$= V^{-1} \frac{2g_n L_z \sqrt{2m}}{2\pi\hbar} \sum_{n=0}^{n_{max}} \left[\epsilon - (n+\frac{1}{2})\hbar\omega_c\right]^{-1/2}, \tag{57}$$

$$= \frac{2eB\sqrt{2m}}{(2\pi\hbar)^2} \sum_{n=0}^{n_{max}} \left[\epsilon - (n+\frac{1}{2})\hbar\omega_c\right]^{-1/2}, \tag{58}$$

$$= \frac{1}{2\pi^2}\left(\frac{2m}{\hbar^2}\right)^{3/2} \frac{\hbar\omega_c}{2} \sum_{n=0}^{n_{max}} \left[\epsilon - (n+\frac{1}{2})\hbar\omega_c\right]^{-1/2}, \tag{59}$$

and n_{max} extends to the maximum Landau level such that the argument of the square-root is positive. We observe that ignoring the discretness of Landau level index n (i.e., in the limit of vanishing $\hbar\omega_c$ ($B \to 0$), i.e., integrating over n, we recover the 3d free-space $g_{3d}(\epsilon) \sim \sqrt{\epsilon}$ result.

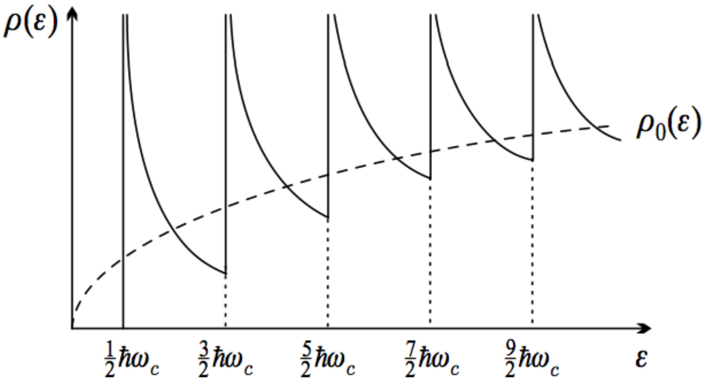

FIG. 12: Density of states of a 3d electron gas in a magnetic field, that at low fields coarse-grains into a 3d $\sqrt{\epsilon}$ form indicated by the dashed curve.[6]

It is this discrete summation over Landau levels that is responsible for periodicity of $\rho_{3d}(\epsilon, B)$ as a function $1/B$ for fixed ϵ_F, corresponding to emptying each Landau level as it passes through the Fermi energy. To see this explicitly we manipulate the density of states using Poisson summation formula, namely that

$$\begin{aligned}\sum_n f(n) &= \int d\sigma \sum_n \delta(\sigma - n) f(\sigma), && (60)\\ &= \int d\sigma \sum_p e^{i2\pi\sigma p} f(\sigma), && (61)\\ &= \sum_p \tilde{f}(2\pi p), && (62)\end{aligned}$$

where $\tilde{f}(p)$ is a Fourier transform of $f(\sigma)$. Utilizing this transformation to perform the sum over n with function $f(n) = 1/\sqrt{\epsilon/\hbar\omega_c - 1/2 - n}$, we find

$$\begin{aligned}g_{3d}(\epsilon, B) &= \frac{1}{4\pi^2}\left(\frac{2m}{\hbar^2}\right)^{3/2} \sqrt{\hbar\omega_c} \sum_{n=0}^{n_{max}} \left[\epsilon/\hbar\omega_c - 1/2 - n\right]^{-1/2}, && (63)\\ &= \frac{1}{4\pi^2}\left(\frac{2m}{\hbar^2}\right)^{3/2} \sqrt{\hbar\omega_c} \sum_p h(p) e^{i2\pi(\epsilon_F/\hbar\omega_c - 1/2)p}, && (64)\end{aligned}$$

which is quite obviously periodic in $\epsilon_F/\hbar\omega_c = B_0/B$, i.e., in $1/B$ with period $1/B_0 = \hbar e/(\epsilon_F m) = 2\pi/(\phi_0 k_F^2)$, corresponding to a change of the argument by an integer, that can be absorbed into shift of n. Above $h(p)$ is Fourier transform of the $1/\sqrt{x}$. Equivalently, the argument of the periodic function can be written as $2\pi p\epsilon_F/\hbar/omega_c = \hbar A_F/(eB)$, where $A_F = \pi k_F^2$ is the Fermi-surface cross-sectional area perpendicular to the applied field $\mathbf{B}$. The periodicity in $1/B$ is then characterized by period $2\pi e/(\hbar A_F)$. This reveals an in important tool for using magnetic field oscillatory response to map out Fermi surface geometry.

At weak fields we can neglect this oscillatory contribution and compute the average uniform part. To see this more explicitly, we calculate the ground-state energy density of the electron gas in the presence of a magnetic field,

$$\mathcal{E}_{FG} = \int_0^{\epsilon_F} \epsilon g(\epsilon) d\epsilon = \frac{1}{2\pi^2}\left(\frac{2m}{\hbar^2}\right)^{3/2} \frac{\hbar\omega_c}{2} \sum_{n=0}^{n_{max}} \int_{(n+1/2)\hbar\omega_c}^{\epsilon_F} \frac{d\epsilon\ \epsilon}{\left[\epsilon - (n+\frac{1}{2})\hbar\omega_c\right]^{1/2}}, \tag{65}$$

Using the Euler-Maclaurin formula $\sum_{n=0}^{n_0} f(n+1/2) = \int_0^{n_0+1} f(x)dx - \frac{1}{24}\left[f'(n_0+1) - f'(0)\right]$ to replace the sum by an integral in a small $\hbar\omega_c$ limit, we find

$$\mathcal{E}_{FG} \approx \frac{3}{5} n\epsilon_F + \frac{1}{24\pi^2}\frac{e^2 k_F}{m} B^2, \tag{66}$$

that leads to magnetization and magnetic susceptibility

$$m = -\frac{\partial \mathcal{E}_{FG}}{\partial B} = -\frac{1}{3}\frac{e^2 k_F}{(2\pi)^2 m} B, \tag{67}$$

$$\chi_{Laundau} = \frac{\partial m}{\partial B} = -\frac{1}{3}\frac{\mu_B^2 k_F m}{\pi^2\hbar^2} = -\frac{1}{3}\mu_B^2 g(\epsilon_F), \tag{68}$$

where in above result we neglected the dependence of ϵ_F on B, that can be shown to be weak and for small fields does not modify above Landau diamagnetism result. Taking $g \approx 2$ demonstrates the result Eq.(50). Combining orbital (Landau) and spin (Pauli) susceptibilities demonstrates that in the $g \approx 2$ approximation the overall susceptibility is indeed paramagnetic. We also note that Landau diamagnetism comes from the Euler-Maclaurin formula correction to the naive replacement of the sum over Landau levels by an integral, thus demonstrating that it is the quantum treatment and discreteness of Landau levels that is responsible for orbital diamagnetism (no classical magnetism).

In the strong field limit, a better approximation beyond Euler-Maclaurin series that includes full discreteness, as computed in Eq.(64) above is necessary. This results in periodicity in the density of states with $1/B$ and then leads to oscillations in a variety of physical quantities, most prominantly the magnetization, (see Fig.(13) the so-called de Haas-van Alphen (dHvA) effect (1930). Other quantities also oscillate, such as the resistivity (Shubnikov-de Haas effect), specific heat, and sound attenuation and speed.

The zero-temperature analysis above is straightforwardly generalized to finite temperature by computing the grand-canonical free energy and differentiating it with respect to B

to obtain $m(B)$ and χ,

$$\Pi_{gr} \;=\; -k_B T \ln Z_{gr} = -k_B T \int_{-\infty}^{\infty} \frac{dk_z}{2\pi} \sum_{n=0,\sigma=\pm 1}^{n_{max}} \frac{1}{2\pi\ell^2} \ln\left[1 + e^{-\beta(\hbar\omega_c(n+1)+\hbar^2 k_z^2/2m+\mu_B B\sigma-\mu)}\right], \tag{69}$$

which gives for $m = -\partial\Pi_{gr}/\partial B$ in the $B \to 0$ limit,

$$m \;=\; \frac{3}{2}\frac{n\mu_B^2}{\epsilon_F}\left[1 - \frac{1}{3} + \frac{\pi k_B T}{\mu_B B}\left(\frac{2\epsilon_F}{\hbar\omega_c}\right)^{1/2} \sum_{p=1}^{\infty} \frac{(-1)^p}{\sqrt{p}} \cos \pi p \, \frac{\sin(\pi/4 - 2\pi p\epsilon_F/\hbar\omega_c)}{\sinh(2\pi^2 p k_B T/\hbar\omega_c)}\right] B, \tag{70}$$

the Lifshitz-Kosevich formula (1954), with the first two constants giving the Pauli (spin) and Landau (orbital) contributions.

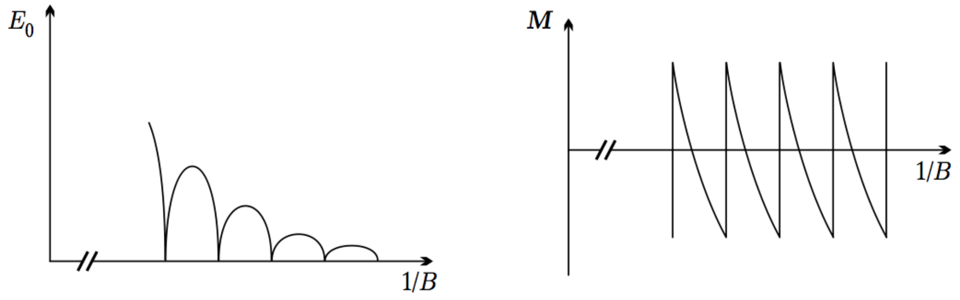

FIG. 13: Ground state energy and magnetization of a two-dimensional electron gas illustrating periodicity as a function of $1/B$.[6]

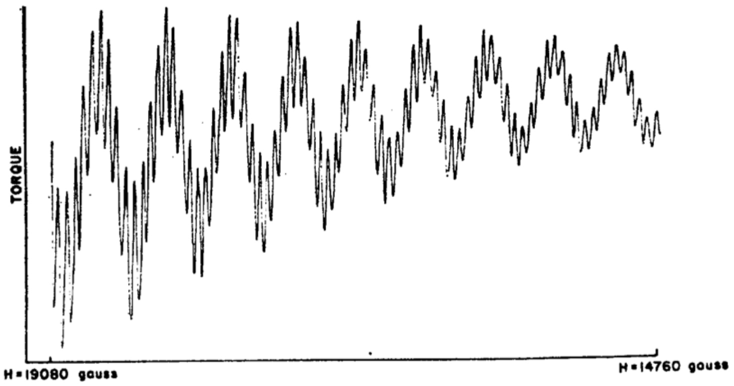

Fig. 22.16. De Haas–van Alphen oscillations in zinc [Reprinted with permission from A. S. Joseph and W. L. Gordon, *Phys. Rev.* **126**, 489 (1962). ©1962 by the American Physical Society]

III. WEAKLY INTERACTING FERMI GAS

A. Greens function preliminaries

Before calculating correlation functions, susceptibilties and effects of interactions for completness it is useful to recall a few properties of fermionic Greens functions.

1. Fermionic Greens functions: canonical formulation

Retarded and advanced Greens functions:

A single noninteracting particle fermionic Greens function at $T = 0$ is easily computed. Let's first consider a retarded Greens function. The usefulness of retarded Greens functions is the fact they are the ones that show up in computation of physical quantities, such as response functions (e.g., conductivity, compressibility, etc...) as we saw in previous section in the RF signal. In vacuum it is given by ($\hbar = 1$)

$$\begin{aligned} G_R^{vac}(k,t) &= -i\theta(t)\langle 0|c_k(t)c_k^\dagger(0)|0\rangle, && (71)\\ &= -i\theta(t)\langle 0|\{c_k(t),c_k^\dagger(0)\}|0\rangle, && (72)\\ &= -i\theta(t)\langle 0|c_k c_k^\dagger|0\rangle e^{-i\epsilon_k t}, && (73)\\ &= -i\theta(t)e^{-i\epsilon_k t}, && (74)\end{aligned}$$

Its Fourier transform is then given by

$$\begin{aligned} G_R^{vac}(k,\omega) &= -i\int_0^\infty dte^{-i\epsilon_k t+i\omega t-\delta t}, && (75)\\ &= \frac{1}{\omega-\epsilon_k+i\delta}, && (76)\end{aligned}$$

and is obviously analytic in the upper-half plane (hence its usefulness); this property is a consequence of the convergent Fourier transform for $Im(\omega) > 0$ and $t > 0$. Similarly, the advanced Greens function is analytic in the lower-half plane and is given by $G_A(\omega) = G_R^*(\omega)$.

We can generalize the vacuum retarded Greens function, above to that for the finite density of fermions. At $T = 0$ just amounts to using the Fermi sea as the ground state and using finite chemical potential, μ. Taking over above vacuum definition, we obtain:

$$\begin{aligned}
G_R^{FS}(k,t) &= -i\theta(t)\langle FS|\{c_k(t), c_k^\dagger(0)\}|FS\rangle, & (77)\\
&= -i\theta(t)\langle FS|c_k c_k^\dagger + c_k^\dagger c_k|FS\rangle e^{-i\varepsilon_k t}, & (78)\\
&= -i\theta(t)e^{-i\varepsilon_k t}, & (79)
\end{aligned}$$

where $\varepsilon_k = \epsilon_k - \mu$ and can therefore be positive (particle excitation) or negative (hole excitation). The corresponding Fourier transform is given by

$$G_R^{FS}(k,\omega) = \frac{1}{\omega - \varepsilon_k + i\delta}, \tag{80}$$

again analytic in the upper-half plane.

Real time-ordered Greens function:

A computationally convenient Greens function (because it appears in the interaction picture perturbation theory and in path integral formulation, where time-ordered correlators come up) is the time-ordered correlation function. It is given by

$$\begin{aligned}
G_T(k,t) &= -i\langle \mathcal{T}_t c_k(t) c_k^\dagger(0)\rangle, & (81)\\
&= -i\theta(t)\langle c_k(t)c_k^\dagger(0)\rangle + i\theta(-t)\langle c_k^\dagger(0)c_k(t)\rangle, & (82)\\
&= -i\theta(t)\langle c_k c_k^\dagger\rangle e^{-i\varepsilon_k t} + i\theta(-t)\langle c_k^\dagger c_k\rangle e^{-i\varepsilon_k t}, & (83)\\
&= -i\theta(t)(1-n_k)e^{-i\varepsilon_k t} + i\theta(-t)n_k e^{-i\varepsilon_k t}. & (84)
\end{aligned}$$

The corresponding Fourier transform (regularizing positive and negative t contributions appropriately with δ) is given by

$$G_T(k,\omega) = \frac{1-n_k}{\omega - \varepsilon_k + i\delta} + \frac{n_k}{\omega - \varepsilon_k - i\delta}, \tag{85}$$

and displays poles in both the upper- and lower-half ω plane for $\varepsilon_k < 0$ and $\varepsilon_k > 0$, respectively. In above $n_k = \langle c_k^\dagger c_k\rangle$, which equals to the Fermi distribution function $n_F(\varepsilon_k) = 1/(e^{\beta\varepsilon_k} + 1)$ at finite T and reduces to $\theta(-\varepsilon_k)$ for $T = 0$. In the latter limit it can be compactly written as

$$G_T(k,\omega) = \frac{1}{\omega - \varepsilon_k + i\delta\, sgn(\varepsilon_k)} \equiv \frac{1}{\omega - \varepsilon_k + i\delta_k}. \tag{86}$$

Note that in the case of a true vacuum state, i.e., $\mu < 0$, $\varepsilon_k > 0$ and $n_k = \theta(-\varepsilon_k) = 0$, reducing G_T to G_R^{vac}.

2. Fermionic Greens functions: coherent states path integral formulation

As we will recall in the next subsection, a convenient way of computing finite temperature real-time response functions is from a corresponding imaginary time-ordered correlation function and then analytically continuing to real frequency via $i\omega_n \rightarrow \omega \pm i\delta$ for retarded and advanced functions, respectively. This is simplifies even $T = 0$ computations and also allows computation of corresponding (non-time-ordered) correlation functions (e.g., frequency dependent structure function) via the fluctuation-dissipation relation.

Consider a fermionic Hamiltonian,

$$H = \int_{\mathbf{r}} \psi^\dagger \hat{\varepsilon} \psi + H_{int}$$

Then the partition function is

$$Z = Tr\left(e^{-\beta H}\right)$$

As usual we can go to coherent states path integral by Trotter decomposition. As for the bosonic coherent path-integral derivation, there will be an overlap between two adjacent coherent states

$$\langle \psi(\tau+\varepsilon)|\psi(\tau)\rangle \;=\; e^{\overline{\psi}(\tau+\varepsilon)\psi(\tau)-\frac{1}{2}\overline{\psi}(\tau+\varepsilon)\psi(\tau+\varepsilon)-\frac{1}{2}\overline{\psi}(\tau)\psi(\tau)}, \tag{87}$$

$$= \; e^{-\overline{\psi}\partial_\tau\psi}, \tag{88}$$

The partition function is then given by

$$Z = \; Z[\overline{\eta}=0, \eta=0] \tag{89}$$

where we introduced a generating function

$$Z[\overline{\eta}, \eta] \;=\; \int \mathcal{D}\overline{\psi}\mathcal{D}\psi e^{-S+\int_{\mathbf{r},\tau}(\overline{\psi}\eta+\overline{\eta}\psi)}, \tag{90}$$

$$\tag{91}$$

convenient for computation of correlation functions. The harmonic ($H_{int} = 0$) action is given by

$$S_0 \;=\; \int_0^\beta d\tau \int_{\mathbf{r}} \overline{\psi}\left(\partial_\tau + \hat{\varepsilon}\right)\psi, \tag{92}$$

$$= \; \sum_{\omega_n}\int_{\mathbf{r}} \overline{\psi}_\omega\left(-i\omega_n + \hat{\varepsilon}\right)\psi_\omega, \tag{93}$$

$$= \; (\beta V)^{-1}\sum_{k,\omega_n} \overline{c}_{\mathbf{k},\omega_n}(-i\omega_n + \varepsilon_k)c_{\mathbf{k},\omega_n}, \tag{94}$$

with the definition of Fourier transform: $\psi(\mathbf{r},\tau) = \frac{1}{V\beta}\sum_{\mathbf{k},\omega_n} c_{\mathbf{k},\omega_n} e^{i\mathbf{k}\cdot\mathbf{r}-i\omega_n\tau}$. The imaginary time τ is related to t by $\tau = it$, and ω_n is the Matsubaru frequency that equals to $2\pi(n+1/2)/\beta$ because of the antisymmetric boundary conditions for fermions, (contrasted with $\omega_n = 2\pi n/\beta$ for bosons) with the antiperiodic Greens function, $G(\tau<0) = -G(\tau+\beta)$. Note that the imaginary time fields "evolve" in τ according to $c(\tau) = e^{H\tau}c(0)e^{-H\tau}$. In second line we used FT convention $\psi(\tau) = \frac{1}{\beta^{1/2}}\sum_{\omega_n}\psi_\omega e^{-i\omega_n\tau}$.

The Grassmann integrals are computed using linearity, anticommutation properties of $\psi, \overline{\psi}$ (treated as independent integration variables), and definitions

$$\int d\psi = 0, \quad \int d\psi\psi = 1,$$

equivalent to differentiation. For a single pair of complex Grassmann variable we have

$$\int d\overline{\psi}d\psi e^{-\overline{\psi}\Gamma\psi} = \int d\overline{\psi}d\psi(1-\overline{\psi}\Gamma\psi) = \Gamma,$$

in contrast to bosonic complex fields where it is $1/\Gamma$. For N decoupled Gaussian integrals defined by Γ_i we get a product $\prod_{i=1}^{N}\Gamma_i$, which generalizes to $\det\Gamma$ for coupled Gaussian variables characterized by matrix Γ_{ij}. By completing the square in the exponential and noting that for Grassman fields $e^{\psi} = 1+\psi$, this leads to

$$\begin{aligned} Z[\overline{\eta},\eta] &= \int \mathcal{D}\overline{\psi}\mathcal{D}\psi e^{-\overline{\psi}_i\Gamma_{ij}\psi_j+\overline{\psi}_i\eta_i+\overline{\eta}_i\psi_i} = \int \mathcal{D}\overline{\psi}\mathcal{D}\psi e^{-(\overline{\psi}_i-\overline{\eta}_l\Gamma^{-1}_{li})\Gamma_{ij}(\psi_j-\Gamma^{-1}_{jk}\eta_k)+\overline{\eta}_i\Gamma^{-1}_{ij}\eta_j}, && (95)\\ &= (\det\Gamma)\, e^{\overline{\eta}_i\Gamma^{-1}_{ij}\eta_j}, && (96) \end{aligned}$$

which by differentiation with respect to $\eta, \overline{\eta}$ gives Wick's theorem.

The fermionic Greens function can now be straightforwardly computed

$$\begin{aligned} G(\omega_n) &= \langle\overline{\psi}\psi\rangle = -\langle\psi\overline{\psi}\rangle, && (97)\\ &= Z^{-1}\int \mathcal{D}\overline{\psi}\mathcal{D}\psi e^{-S}\overline{\psi}\psi = \frac{\delta}{\delta\overline{\eta}}\frac{\delta}{\delta\eta}\ln Z[\overline{\eta},\eta]_{\eta,\overline{\eta}=0} = -\frac{\delta}{\delta\eta}\frac{\delta}{\delta\overline{\eta}}\ln Z[\overline{\eta},\eta]_{\eta,\overline{\eta}=0}, && (98)\\ &= -\int \mathcal{D}\overline{\psi}\mathcal{D}\psi e^{-\sum_{\omega_n}\overline{\psi}_\omega(-i\omega_n+\varepsilon)\psi_\omega}\psi\overline{\psi}, && (99)\\ &= -\frac{\delta}{\delta\eta}\frac{\delta}{\delta\overline{\eta}}e^{\sum_{\omega_n}\overline{\eta}\frac{1}{-i\omega_n+\varepsilon}\eta}|_{\eta,\overline{\eta}=0} = -\frac{\delta}{\delta\eta}\frac{\delta}{\delta\overline{\eta}}\overline{\eta}\frac{1}{-i\omega_n+\varepsilon}\eta|_{\eta,\overline{\eta}=0}, && (100)\\ &= \frac{1}{i\omega_n-\varepsilon}. && (101) \end{aligned}$$

Analytic continuation to real frequencies via $i\omega_n \to \omega + i0^+$ gives retarded Greens function

$$G_R(\omega) = \frac{1}{\omega-\varepsilon+i0^+}, \tag{102}$$

that is analytic in the upper-half plane. Notice that it is distinct from the real-time ordered Greens function, (85)

In time domain, the Greens function is time-ordered and is given by

$$
\begin{aligned}
G_T(\tau) &= -\langle \mathcal{T}_\tau \hat{\psi}(\tau)\hat{\psi}^\dagger(0)\rangle = -\langle \mathcal{T}_\tau \psi(\tau)\overline{\psi}(0)\rangle, &(103)\\
&= -\theta(\tau)\langle \hat{\psi}(\tau)\hat{\psi}^\dagger(0)\rangle + \theta(-\tau)\langle \hat{\psi}^\dagger(0)\hat{\psi}^\dagger(\tau)\rangle. &(104)
\end{aligned}
$$

Let us check that calculating its Matsubaru Fourier transform in operator form (as in real time in (84)) indeed gives the simple form (101). In momentum **k**-space, we have

$$
\begin{aligned}
G_T(\mathbf{k},\tau) &= -\langle \mathcal{T}_\tau c_{\mathbf{k}}(\tau) c^\dagger_{\mathbf{k}}(0)\rangle, &(105)\\
&= -\theta(\tau)\langle c_{\mathbf{k}}(\tau)c^\dagger_{\mathbf{k}}(0)\rangle + \theta(-\tau)\langle c^\dagger_{\mathbf{k}}(0)c_{\mathbf{k}}(\tau)\rangle, &(106)\\
&= -\theta(\tau)\langle c_{\mathbf{k}}c^\dagger_{\mathbf{k}}\rangle e^{-\varepsilon_k\tau} + \theta(-\tau)\langle c^\dagger_{\mathbf{k}}c_{\mathbf{k}}\rangle e^{-\varepsilon_k\tau}, &(107)\\
&= -\theta(\tau)(1-n_F(\varepsilon_k))e^{-\varepsilon_k\tau} + \theta(-\tau)n_F(\varepsilon_k)e^{-\varepsilon_k\tau}, &(108)
\end{aligned}
$$

where in the last line we used thermal average in the grand-canonical ensemble

$$
\begin{aligned}
\langle c^\dagger_{\mathbf{k}}c_{\mathbf{k}}\rangle &= Z_{gr}^{-1}\mathrm{Tr}\left[e^{-\beta\hat{H}_\mu}c^\dagger_k c_k\right] = n_F(\varepsilon_k) = \frac{1}{e^{\beta\varepsilon_k}+1}, &(109)\\
\langle c_{\mathbf{k}}c^\dagger_{\mathbf{k}}\rangle &= 1-\langle c^\dagger_{\mathbf{k}}c_{\mathbf{k}}\rangle = 1-n_F(\varepsilon_k) = \frac{1}{e^{-\beta\varepsilon_k}+1}, &(110)
\end{aligned}
$$

Matsubaru Fourier-transforming $G_T(k,\tau)$

$$
\begin{aligned}
G_T(k,\omega_n) &= \int_0^\beta d\tau G_T(\mathbf{k},\tau)e^{i\omega_n\tau}, &(111)\\
&= \int_0^\beta d\tau\left[-\theta(\tau)(1-n_F(\varepsilon_k))+\theta(-\tau)n_F(\varepsilon_k)\right]e^{-\varepsilon_k\tau}e^{i\omega_n\tau}, &(112)\\
&= -\int_0^\beta d\tau(1-n_F(\varepsilon_k))e^{(i\omega_n-\varepsilon_k)\tau}, &(113)\\
&= -\frac{1-n_F(\varepsilon_k)}{i\omega_n-\varepsilon_k}\left[e^{(i\omega_n-\varepsilon_k)\beta}-1\right] = -\frac{1-n_F(\varepsilon_k)}{i\omega_n-\varepsilon_k}\left[-e^{-\varepsilon_k\beta}-1\right], &(114)\\
&= \frac{1}{i\omega_n-\varepsilon_k}, &(115)
\end{aligned}
$$

which reassuringly indeed gives (101). When analytically continued it also gives the retarded Greens function in (102). On the other hand, notice that if we first analytically continue $G_T(\tau)$ in time, namely, $G_T(\tau)\to iG_T(it)$, and then Fourier transform to real frequencies we get the Fourier-transform of time-ordered (not retarded) Greens function, (85).

Let us check that this Greens function gives the correct fermion density. Note that for positive (negative) τ the contour must be closed in the lower-half (upper-half) plane (so that the result is convergent at large imaginary $\omega = \pm ia$). So for $\tau < 0$, we must close the contour in the upper-half plane, but the pole is at $\omega = -i\varepsilon_k$, i.e., in the upper-half plane for $k < k_F$ ($\varepsilon_k < 0$) and in the lower-half plane for $k > k_F$ ($\varepsilon_k < 0$). With this we obtain the fermion density

$$
\begin{aligned}
n &= \langle\overline{\psi}(0)\psi(0^-)\rangle = G(\tau \to 0^-), && (116)\\
&= V^{-1}\sum_{\mathbf{k}}\int\frac{d\omega}{2\pi}\frac{e^{-i\omega\tau}}{i\omega - \varepsilon_k}, && (117)\\
&= \int_{\mathbf{k}}\theta(-\varepsilon_k), && (118)
\end{aligned}
$$

that is consistent with the standard result of the $T = 0$ Fermi function for the Fermi gas. At finite temperature we instead sum over Matzubaru frequencies obtaining $\theta(-\varepsilon_k) \to n_F(\varepsilon_k)$.

Note that the chosen V and β factors in the Fourier transform give a well defined continuum limits: $1/(V\beta)\sum_{k,\omega_n}\ldots = (2\pi)^{-(d+1)}\int d\omega d^dk\ldots$. Also, division by βV in the definition of the Fourier-transformed correlation function corresponds to cancelling out the frequency and momentum conserving δ-functions.

We note that computation of Greens function in imaginary time do not require large τ regularization as poles are automatically off the real axis. Also, the time-ordering is done automatically through the path integral, that is always time-ordered, by definition. Finally, we note that above mentioned analytical continuation to real frequencies, $\omega_n \to \omega \pm i\delta$, automatically gives the advanced and retarded Greens functions that are commutators and anticommutators for bosons and fermions, respectively, not the real time ordered correlation functions. To get the latter, one can either analytically continuum to real time and then Fourier transform or instead use fluctuation-dissipation relation (see below).

3. *Spectral decomposition and Kramer-Kronig relation:*

Below we recall a few other relations that we will find useful. Lehmann's spectral decomposition expresses the retarded Greens function in terms of its imaginary part, i.e., its spectral function,

$$G_R(i\omega_n) \;=\; \int_{-\infty}^{\infty} \frac{d\nu}{2\pi i} \frac{G_R(\nu) - G_R(-\nu)}{\nu - i\omega_n}, \tag{119}$$

$$\;=\; \int_{-\infty}^{\infty} \frac{d\nu}{\pi} \frac{G_R''(\nu)}{\nu - i\omega_n}. \tag{120}$$

Above relation is seen to be true by closing the contour in the upper- and lower-half planes for $G_R(\nu)$ and $G_R(-\nu)$, where each is analytic, respectively, noting that the first (second) term vanishes for $\omega_n < 0$ $(\omega_n > 0)$.

Kramer-Kronig relation follows directly from the spectral decomposition above by analytically continuing to real frequencies and taking a real part of both sides

$$G_R'(\omega) = P\int_{-\infty}^{\infty} \frac{d\nu}{\pi} \frac{G_R''(\nu)}{\nu - \omega}, \tag{121}$$

where P stands for a principle part regularization of the integral. Note also imaginary part of both sides of Eq.(120) automatically satisfies the equation, using $1/(x - i0) = P(1/x) + i\pi\delta(x)$. Equivalently, the K-K relation can be derived by noting that

$$\int_{-\infty}^{\infty} d\nu \frac{G_R(\nu)}{\nu - \omega + i\delta} \;=\; 0, \tag{122}$$

by closing the contour in the upper-half plane where $G_R(\nu)$ is analytic. Then using the real and imaginary decomposition for $1/(\nu - \omega + i\delta) = P(1/(\nu - \omega)) - i\pi\delta(\nu - \omega)$, we find

$$P\int_{-\infty}^{\infty} d\nu \frac{G_R(\nu)}{\nu - \omega} = i\pi G_R(\omega), \tag{123}$$

whose imaginary part gives K-K, above; the real part gives the complementary form of K-K. Equivalently, $\delta \longrightarrow 0$ limit can be taken and contour along real axis completed by a semi-circle above and below the real axis to avoid the pole at ω. The contour integral along the real axis then gives the principle part and around semi-circular contour gives $-i\pi G_R(\omega)$ (when it lies in upper-half plane), giving the same result as above.

It is also convenient to introduce a spectral function

$$A(k,\omega) \;=\; -2G_R''(k,\omega), \tag{124}$$

that for a free particle is given by $A_0(k,\omega) = 2\pi\delta(\omega - \varepsilon_k)$, as can be seen by using (102) and taking its imaginary part. $A(k,\omega)$ allows us to express the corresponding retarded Greens function in terms of a frequency integral over the spectral function, as can be seen from Lehmann spectral representation above, that gives

$$G_R(\mathbf{k}, i\omega_n) \; = \; \int_{-\infty}^{\infty} \frac{d\nu}{2\pi} \frac{A(\mathbf{k},\nu)}{i\omega_n - \nu}. \tag{125}$$

Simple analysis on Eq.(125) (summing over ω_n) shows that the occupation function and the density of states are given by

$$n_k \; = \; \int_{-\infty}^{\infty} \frac{d\omega}{2\pi} A(k,\omega) n_F(\omega), \tag{126}$$

$$\rho(\omega) \; = \; \sum_k A(k,\omega). \tag{127}$$

We also note an important sum rule

$$\int_{-\infty}^{\infty} \frac{d\omega}{2\pi} A(k,\omega) = 1. \tag{128}$$

4. Relation between imaginary time (thermal Matsubara) and real-time retarded Greens functions

We can use spectral decomposition to demonstrate an important relation between imaginary-time time-ordered correlation functions and real-time retarded Greens functions.

For fermions we have:

$$\begin{aligned} G_R(k,t) \; &= \; -i\theta(t)V^{-1}\text{Trace}\big[\rho\{c_k(t), c_k^\dagger(0)\}\big], &(129)\\ &= \; -i\theta(t)(VZ_{gc})^{-1}\sum_n \langle n|c_k(t)c_k^\dagger(0) + c_k^\dagger(0)c_k(t)|n\rangle e^{-\beta E_n}, &(130)\\ &= \; -i\theta(t)(VZ_{gc})^{-1}\sum_{n,m}\left[|\langle n|c_k|m\rangle|^2 e^{i(E_n-E_m)t} + |\langle m|c_k|n\rangle|^2 e^{-i(E_n-E_m)t}\right]e^{-\beta E_n}, &(131)\\ &= \; -i\theta(t)(VZ_{gc})^{-1}\sum_{n,m}|\langle n|c_k|m\rangle|^2 e^{i(E_n-E_m)t}\big(e^{-\beta E_n} + e^{-\beta E_m}\big), &(132) \end{aligned}$$

where $\rho = e^{-(H-\mu N)}/Z_{gc}$ is the equilibrium grand-canonical density matrix (in Schrodinger representation), Z_{gc} is the grand-canonical partition function, giving the free energy via $Z_{gc} = e^{-\beta F}$, $|n\rangle$ are the exact eigenstates of $H_\mu = H - \mu N$, with eigenvalues E_n.

Fourier transforming in time, gives

$$G_R(k,\omega) \; = \; (VZ_{gc})^{-1}\sum_{n,m}\frac{|\langle n|c_k|m\rangle|^2\big(e^{-\beta E_n} + e^{-\beta E_m}\big)}{\omega + E_n - E_m + i\delta}, \tag{133}$$

where $i\delta$ was added to ensure convergence at large $t \to +\infty$.

We now show that $G_R(\omega)$ can be equivalently obtained from Fourier transform of imaginary-time ordered correlation function via analytical continuation $\omega_n \to \omega + i\delta$. To see this consider

$$\begin{aligned}
G_\tau(\tau) &= -\frac{1}{V}\langle \mathcal{T}_\tau c(\tau) c^\dagger(0)\rangle, && (134)\\
&= -\frac{\theta(\tau)}{V}\langle c(\tau)c^\dagger(0)\rangle + \frac{\theta(-\tau)}{V}\langle c^\dagger(0)c(\tau)\rangle, && (135)\\
&= -\frac{1}{VZ_{gc}}\sum_n \langle n|\theta(\tau)c_k(\tau)c_k^\dagger(0) - \theta(-\tau)c_k^\dagger(0)c_k(\tau)|n\rangle e^{-\beta E_n}, && (136)\\
&= -\frac{1}{VZ_{gc}}\sum_{n,m}\left[\theta(\tau)\langle n|e^{H_\mu\tau}c_k e^{-H_\mu\tau}|m\rangle\langle m|c_k^\dagger|n\rangle - \theta(-\tau)\langle n|c_k^\dagger|m\rangle\langle m|e^{H_\mu\tau}c_k e^{-H_\mu\tau}|n\rangle\right]e^{-\beta E_n}, && (137)\\
&= -\frac{1}{VZ_{gc}}\sum_{n,m}\left[\theta(\tau)|\langle n|c_k|m\rangle|^2 e^{(E_n-E_m)\tau} - \theta(-\tau)|\langle m|c_k|n\rangle|^2 e^{(E_m-E_n)\tau}\right]e^{-\beta E_n}, && (138)
\end{aligned}$$

Fourier transforming, we obtain:

$$\begin{aligned}
G_\tau(\omega_n) &= \int_0^\beta d\tau G_\tau(\tau), && (139)\\
&= -\frac{1}{VZ_{gc}}\sum_{n,m}|\langle n|c_k|m\rangle|^2 \frac{e^{\beta(E_n-E_m)+i\omega_n\beta}-1}{i\omega_n+E_n-E_m}e^{-\beta E_n}, && (140)\\
&= \frac{1}{VZ_{gc}}\sum_{n,m}|\langle n|c_k|m\rangle|^2 \frac{e^{-\beta E_m}+e^{-\beta E_n}}{i\omega_n+E_n-E_m}. && (141)
\end{aligned}$$

Note that $\theta(-\tau)$ term does not contribute to the Fourier transform. Also, we used the fact that $e^{i\omega_n\beta} = -1$ for fermionic ω_n. Thus, comparing Eqs.(133) and (141), we indeed find that the former can be obtained from the latter via analytical continuation $i\omega_n \to \omega + i\delta$.

We further note that $G_R(\mathbf{k}, \omega)$ can be expressed in terms of an integral over its imaginary part, namely the spectral function defined in Eq.(124)

$$\begin{aligned}
A(k,\omega) &= -2G_R''(k,\omega), && (142)\\
&= \frac{1}{VZ_{gc}}\sum_{n,m}|\langle n|c_k|m\rangle|^2 e^{-\beta E_m}\left(1+e^{\beta(E_m-E_n)}\right)2\pi\delta(\omega-(E_m-E_n)), && (143)\\
&= \frac{n_F(\omega)^{-1}}{VZ_{gc}}\sum_{n,m}|\langle n|c_k|m\rangle|^2 e^{-\beta E_m}2\pi\delta(\omega-(E_m-E_n)). && (144)
\end{aligned}$$

giving

$$\begin{aligned}
G_R(\omega) &= \int_{-\infty}^{\infty}\frac{d\nu}{2\pi}\frac{A(k,\nu)}{\omega-\nu}, && (145)\\
& && (146)
\end{aligned}$$

From the expression for $A(k,\omega)$ we also find a useful expression for the occupation function

$$\begin{aligned} n_k &= \frac{1}{VZ_{gc}}\sum_m \langle m|c_k^\dagger c_k|m\rangle e^{-\beta E_m}, && (147)\\ &= \frac{1}{VZ_{gc}}\sum_{n,m} |\langle n|c_k|m\rangle|^2 e^{-\beta E_m}, && (148)\\ &= \int \frac{d\nu}{2\pi} A(k,\nu) n_F(\nu). && (149)\end{aligned}$$

In imaginary time formalism n_k can be computed from the imaginary-time-ordered correlation function. For a free fermion it is given by:

$$\begin{aligned} n_k &= \text{Trace}\left[c_k^\dagger c_k e^{-\beta H_\mu}\right], && (150)\\ &= \langle \mathcal{T}_\tau c_k^\dagger(0^+) c_k(0)\rangle, && (151)\\ &= \sum_{\omega_n} \frac{e^{i\omega_n 0^+}}{i\omega_n - \varepsilon_k}, && (152)\\ &= n_F(\varepsilon_k) =_{T\to 0} \theta(-\varepsilon_k), && (153)\\ &= \int \frac{d\nu}{2\pi} n_F(\nu) 2\pi\delta(\nu - \varepsilon_k). && (154)\end{aligned}$$

Above analysis can be repeated for bosonic operators, with differences being that the retarded propagator is a commutator (rather than fermionic anticommutator) and time-ordered correlator has a relative plus (rather than fermionic minus) sign between $\theta(\tau)$ and $\theta(-\tau)$, with these leading to replacement of $n_F(\omega)$ to $n_B(\omega)$.

We can also use this spectral decomposition to establish a general relation between real-time (non-time-ordered) correlation function and retarded propagator, i.e., fluctuation-dissipation (Kubo) relations. In physical contexts these correlation functions relations arise for bosonic operators (e.g., current in the case of conductivity and density in the case of compressibility and dynamic structure function relation). Thus we will derive these relations for a bosonic operator.

To this end, consider density-density correlation function

$$\begin{aligned} S(k,t) &= V^{-1}\langle \rho_k(t)\rho_{-k}(0)\rangle, && (155)\\ &= \frac{1}{VZ_{gc}}\sum_n \langle n|e^{iHt}\rho_k e^{-iHt}\rho_{-k}|n\rangle e^{-\beta E_n}, && (156)\\ &= \frac{1}{VZ_{gc}}\sum_{n,m} |\langle n|\rho_k|m\rangle|^2 e^{-\beta E_n + i(E_m - E_n)t}, && (157)\end{aligned}$$

whose real-time Fourier transform is the dynamic structure function and is given by:

$$S(k,\omega) \;=\; \frac{1}{VZ_{gc}}\sum_{n,m}|\langle n|\rho_k|m\rangle|^2 e^{-\beta E_n}2\pi\delta(\omega - E_m + E_n). \tag{158}$$

We now use spectral decomposition to compute the imaginary-time-ordered correlator of $\rho_k(\tau)$ (corresponding to the above dynamic structure function) and via analytical continuation, $i\omega_n \to \omega + i\delta$ obtain the density response function, given by the retarded correlation function:

$$\chi(k,\tau) \;=\; -V^{-1}\langle \mathcal{T}_\tau \rho_k(\tau)\rho_{-k}(0)\rangle, \tag{159}$$

$$\;=\; -\frac{\theta(\tau)}{V}\langle \rho_k(\tau)\rho_{-k}(0)\rangle - \frac{\theta(-\tau)}{V}\langle \rho_{-k}(0)\rho_k(\tau)\rangle, \tag{160}$$

$$\;=\; -\frac{1}{VZ_{gc}}\sum_n \langle n|\theta(\tau)\rho_k(\tau)\rho_{-k}(0) + \theta(-\tau)\rho_{-k}(0)\rho_k(\tau)|n\rangle e^{-\beta E_n}, \tag{161}$$

$$\;=\; -\frac{1}{VZ_{gc}}\sum_{n,m}\Big[\theta(\tau)\langle n|e^{H_\mu\tau}\rho_k e^{-H_\mu\tau}|m\rangle\langle m|\rho_{-k}|n\rangle + \theta(-\tau)\langle n|\rho_{-k}|m\rangle\langle m|e^{H_\mu\tau}\rho_k e^{-H_\mu\tau}|n\rangle\Big]e^{-\beta E_n}, \tag{162}$$

$$\;=\; -\frac{1}{VZ_{gc}}\sum_{n,m}\Big[\theta(\tau)|\langle n|\rho_k|m\rangle|^2 e^{(E_n-E_m)\tau} + \theta(-\tau)|\langle m|\rho_k|n\rangle|^2 e^{(E_m-E_n)\tau}\Big]e^{-\beta E_n}, \tag{163}$$

Fourier transforming, we obtain

$$\chi(\omega_n) \;=\; \int_0^\beta d\tau \chi(\tau) e^{i\omega_n\tau}, \tag{164}$$

$$\;=\; -\frac{1}{VZ_{gc}}\sum_{n,m}|\langle n|\rho_k|m\rangle|^2 \frac{e^{\beta(E_n-E_m)+i\omega_n\beta} - 1}{i\omega_n + E_n - E_m}e^{-\beta E_n}, \tag{165}$$

$$\;=\; \frac{1}{VZ_{gc}}\sum_{n,m}|\langle n|\rho_k|m\rangle|^2 \frac{e^{-\beta E_n} - e^{-\beta E_m}}{i\omega_n + E_n - E_m}, \tag{166}$$

where we used the fact that $e^{i\omega_n\beta} = 1$ for bosonic ω_n. Analytically continuing to real frequencies, we obtain the (retarded) response function:

$$\chi(\omega) \;=\; \int_{-\infty}^{\infty} dt e^{i\omega t}\chi_R(t), \tag{167}$$

$$\;=\; -i(Z_{gc}V)^{-1}\int_{-\infty}^{\infty} dt e^{i\omega t}\theta(t)\mathrm{Trace}\Big(e^{-\beta H}[\rho_k(t),\rho_{-k}(0)]\Big), \tag{168}$$

$$\;=\; \frac{1}{VZ_{gc}}\sum_{n,m}|\langle n|\rho_k|m\rangle|^2 \frac{e^{-\beta E_n} - e^{-\beta E_m}}{\omega + E_n - E_m + i\delta}, \tag{169}$$

whose imaginary part is clearly related to the dynamic structure function via quantum fluctuation-dissipation relation:

$$2\mathrm{Im}\chi(k,\omega) = (1 - e^{-\beta\omega})S(k,\omega). \tag{170}$$

As a check, this reduces to the standard classical FDT

$$\frac{2T}{\omega}\mathrm{Im}\chi(k,\omega) = S(k,\omega). \tag{171}$$

in the $\omega/T \ll 1$ limit, easily obtained from corresponding Langevin equation with noise that satisfies FDT.

We note that this automatically gives the detailed-balanced Boltzmann ratio for emission and absorption (of e.g., phonon or other quanta). That is for negative ω (emission) the amplitude of the $S(k,\omega)$ peak is $1/(e^{\beta|\omega|}-1)$, which is suppressed compared to positive ω (absorption) amplitude that is proportional to $e^{\beta\omega}/(e^{\beta\omega}-1)$. Thus the ratio of emission at ω to absorption at ω is $e^{-\beta|\omega|}$.

5. *Density response function of a noninteracting Fermi gas density*

Let us now compute density response function for a noninteracting Fermi gas. As established above, this can be done by computing the imaginary-time-ordered correlation function and then analytically continuing it to real frequencies,

$$\begin{align}
\chi_0(\omega_n,\mathbf{k}) &= -\langle\overline{\psi}\psi\overline{\psi}'\psi'\rangle|_{\omega_n,\mathbf{k}}, \tag{172}\\
&= \langle\overline{\psi}\psi'\rangle\langle\overline{\psi}'\psi\rangle|_{\omega_n,\mathbf{k}}, \tag{173}\\
&= \int_{\tau,\mathbf{r}} G(\tau,\mathbf{r})G(-\tau,-\mathbf{r})e^{i\omega_n\tau-i\mathbf{k}\cdot\mathbf{r}}, \tag{174}\\
&= \int_{\nu,\mathbf{q}} G(\nu,\mathbf{q})G(\nu-\omega_n,\mathbf{q}-\mathbf{k}), \tag{175}\\
&= \int_{\nu,\mathbf{q}} \frac{1}{(i\nu-\varepsilon_{\mathbf{q}})(i(\nu-\omega_n)-\varepsilon_{\mathbf{q}-\mathbf{k}})}, \tag{176}\\
&= \frac{2\pi i}{2\pi i}\int_{\mathbf{q}}\left[\frac{\theta(\varepsilon_{\mathbf{q}})\theta(-\varepsilon_{\mathbf{q}-\mathbf{k}})}{i\omega_n+\varepsilon_{\mathbf{q}-\mathbf{k}}-\varepsilon_{\mathbf{q}}} + \frac{\theta(-\varepsilon_{\mathbf{q}})\theta(\varepsilon_{\mathbf{q}-\mathbf{k}})}{-i\omega_n+\varepsilon_{\mathbf{q}}-\varepsilon_{\mathbf{q}-\mathbf{k}}}\right], \tag{177}\\
&= -\int_{\mathbf{q}}\frac{\theta(-\varepsilon_{\mathbf{q}})[1-\theta(-\varepsilon_{\mathbf{q}-\mathbf{k}})]-[1-\theta(-\varepsilon_{\mathbf{q}})]\theta(-\varepsilon_{\mathbf{q}-\mathbf{k}})}{i\omega_n+\varepsilon_{\mathbf{q}-\mathbf{k}}-\varepsilon_{\mathbf{q}}}, \tag{178}\\
&= -\int_{\mathbf{q}}\frac{\theta(-\varepsilon_{\mathbf{q}})-\theta(-\varepsilon_{\mathbf{q}-\mathbf{k}})}{i\omega_n+\varepsilon_{\mathbf{q}-\mathbf{k}}-\varepsilon_{\mathbf{q}}}, \tag{179}\\
&= -\int\frac{d^d\mathbf{q}}{(2\pi)^d}\frac{n_F(\varepsilon_{\mathbf{q}})-n_F(\varepsilon_{\mathbf{q}-\mathbf{k}})}{i\omega_n+\varepsilon_{\mathbf{q}-\mathbf{k}}-\varepsilon_{\mathbf{q}}}, \tag{180}
\end{align}$$

where the theta-functions encode that terms appear only when poles are of particular sign and therefore reside on the correct side of the real axis, and in the last line we generalize to finite T in an obvious way. At $T = 0$ the response is nonzero only in two cases (i) $k < q_F$, $|\mathbf{q} - \mathbf{k}| > q_F$, and (ii) $k > q_F$, $|\mathbf{q} - \mathbf{k}| < q_F$, corresponding to electron-hole excitations with electron (hole) above (below) Fermi sea.

After analytical continuation to real frequencies $i\omega_n \to \omega + i0^+$, $\chi(\omega_n, \mathbf{k})$ encodes the density response function

$$\chi_{sc}(\omega, \mathbf{k}) = -i \int_{-\infty}^{\infty} dt e^{i\omega t} \theta(t) \langle [n_k(t), n_{-k}(0)] \rangle,$$

to an external scalar potential, in the uniform limit a response to the chemical potential, namely the compressibility. In the second line, above, we exchanged fermionic fields to apply Wick's contraction, thereby picking up an additional minus sign.

$\chi_0(\omega, \mathbf{k})$ can now be straightforwardly evaluated at $T = 0$. In 3d, to do the $\mathbf{q}$ integral, we analytically continue to real frequencies, shift the variables of integration and then choose z-axis to be along $\mathbf{k}$ and perform the integral in Cartesian coordinates, obtaining

$$\chi_0(\omega, \mathbf{k}) = -\int_{-q_F}^{q_F} dq_z \int \frac{d^2\mathbf{q}_\perp}{(2\pi)^3} \left[\frac{1}{\omega - q_z k/m + k^2/2m + i0^+} - \frac{1}{\omega - q_z k/m - k^2/2m + i0^+} \right], \tag{181}$$

$$= -\int_{-q_F}^{q_F} dq_z \frac{\pi(q_F^2 - q_z^2)}{(2\pi)^3} \left[\frac{1}{\omega - q_z k/m + k^2/2m + i0^+} - \frac{1}{\omega - q_z k/m - k^2/2m + i0^+} \right], \tag{182}$$

$$\begin{aligned} &= -\frac{q_F m}{4\pi^2} - \frac{1}{8\pi^2} \left(\frac{m}{k} \right)^3 \left[\left(\frac{k^2 q_F^2}{m^2} - (\omega + k^2/2m)^2 \right) \ln \left(\frac{\omega + k^2/2m + kq_F/m + i0^+}{\omega + k^2/2m - kq_F/m + i0^+} \right) \right. \\ &\quad \left. + \left(\frac{k^2 q_F^2}{m^2} - (\omega - k^2/2m)^2 \right) \ln \left(\frac{\omega - k^2/2m - kq_F/m + i0^+}{\omega - k^2/2m + kq_F/m + i0^+} \right) \right] \end{aligned} \tag{183}$$

The density susceptibility, $\chi_{sc}(\omega, \mathbf{k})$ also gives the dielectric function via

$$\epsilon(\omega, \mathbf{k}) = 1 - \frac{4\pi e^2}{k^2} \chi_{sc}(\omega, \mathbf{k}), \tag{184}$$

that in the static $\omega \to 0$ and $\mathbf{k} \to 0$ limits gives $\chi_0(0,0) = -\frac{q_F m}{4\pi^2} \equiv -\frac{k_{TF}^2}{4\pi e^2}$, with $k_{TF}^2 = \frac{3\pi e^2 n_0}{\epsilon_F} = 4\pi e^2 g(\epsilon_F)$, $n_0 = q_F^3/(6\pi^2)$, which leads to Thomas-Fermi screening, $V(k) = 4\pi e^2/(\epsilon(k)k^2) = e^2/(k^2 + k_{TF}^2)$.

At finite frequency and $k \to 0$, this function also gives $\epsilon(\omega, 0) = 1 - \omega_p^2/\omega^2$, with the plasmon frequency given by $\omega_p^2 = 4\pi n e^2/m \sim \sqrt{e^2 q_F \epsilon_F} \sim \epsilon_F \sqrt{r_s}$. Note that the imaginary parts of χ_0, involve argument of the logarithmic function and give either 0 or π given the infinitesimal $i0^+$.

The behavior of imaginary part of $\chi_0(\omega, \mathbf{k})$ depends strongly on the regime of $\omega, \mathbf{k}$, determined by whether the frequency falls into the 2-particle continuum, bounded by two curves:

$\omega < k^2/2m \pm kq_F$, technically distinguished by the phase of the argument of the logarithms being 0 or π:

- $k > 2q_F$
    - $0 < \omega < k^2/2m - kq_F/m$:

      $Im(\chi_0) = 0$
    - $k^2/2m - kq_F/m < \omega < k^2/2m + kq_F/m$:

      $Im(\chi_0) = \frac{m}{8\pi k}\left[q_F^2 - \frac{m^2}{k^2}(\omega - k^2/2m)^2\right]$
    - $\omega > k^2/2m + kq_F/m$:

      $Im(\chi_0) = 0$
- $k < 2q_F$
    - $0 < \omega < kq_F/m - k^2/2m$

      $Im(\chi_0) = \frac{m^2}{4\pi}\frac{\omega}{k}$
    - $kq_F/m - k^2/2m < \omega < k^2/2m + kq_F/m$:

      $Im(\chi_0) = \frac{m}{8\pi k}\left[q_F^2 - \frac{m^2}{k^2}(\omega - k^2/2m)^2\right]$
    - $\omega > k^2/2m + kq_F/m$:

      $Im(\chi_0) = 0$

We note that despite a qualitative change in form between first two regimes for $k < 2q_F$, $\chi_0''(\omega, \mathbf{k})$ is indeed continuous across the dotted curve (see Fig.(21)).

In the static limit $\omega = 0$, we find the standard result (Lindhardt dielectric function)

$$\chi_0(0,\mathbf{k}) = -\frac{q_F m}{4\pi^2} - \frac{1}{4\pi^2}\left(\frac{m}{k}\right)^3\left[\left(\frac{k^2 q_F^2}{m^2} - (k^2/2m)^2\right)\ln\left|\frac{k^2/2m + kq_F/m}{k^2/2m - kq_F/m}\right|\right], \tag{185}$$

$$= -\frac{1}{8\pi^2}\frac{q_F^3}{\varepsilon_F}\left[1 + \frac{1}{2x}(1 - x^2)\ln\left|\frac{1+x}{1-x}\right|\right], \tag{186}$$

$$\tag{187}$$

where $x = k/2k_F$, proportional to the density of states n/ϵ_F. For small k ($x \to 0$) the function is well behaved, going as $-\frac{k_{TF}^2}{4\pi e^2}(1 - x^2/3 + O(x^4))$, and giving $k_{TF}^2/(4\pi e^2)$ for $k = 0$.

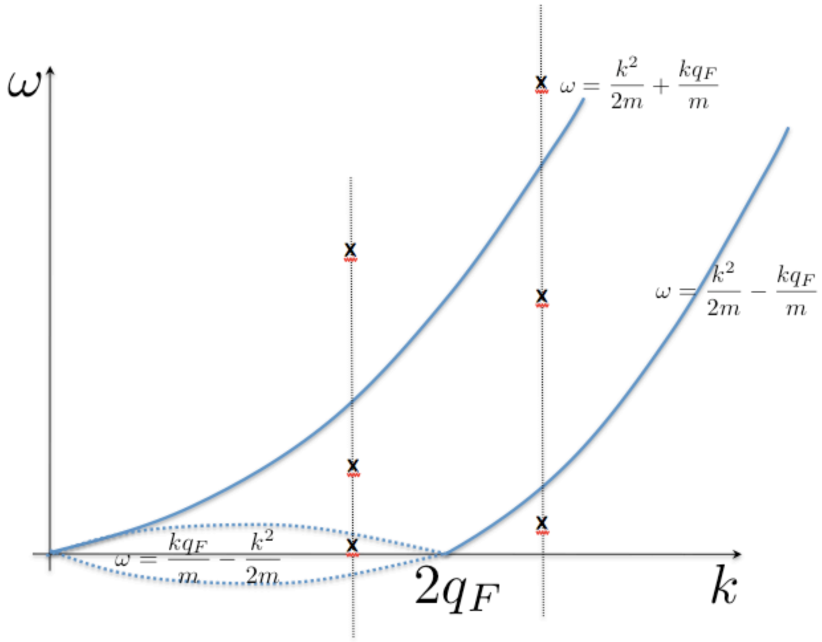

FIG. 14: Two-particle continuum and corresponding regions of distinct behavior of $\chi_0(\omega, k)$ marked by ×'s. As discussed in detail in the text, the imaginary part of the density response function, $\chi_0''(\omega, k)$ is nonzero only between the full lines. There is a change in the behavior of $\chi_0''(\omega, k)$ across the dotted line.

B. Interacting electron gas

1. *Many-body model Hamiltonian*

We now are finally ready to analyze the behavior of a Fermi gas, interacting with Coulomb interactions

$$H_{el} = H_0 + H_{int} = \sum_i^N \frac{\hat{\mathbf{p}}_i^2}{2m} + \frac{1}{2}\sum_{i\neq j}^N \frac{e^2}{|\mathbf{r}_i - \mathbf{r}_j|}, \tag{188}$$

where we neglected the interaction with the ions, the spin-orbit interaction and for now focussed on zero electromagnetic field. The corresponding many-body Hamiltonian is given by

$$\begin{aligned} H_{el} &= \int_{\mathbf{r}} \psi_\sigma^\dagger \frac{-\hbar^2\nabla^2}{2m}\psi_\sigma + \frac{1}{2}\int_{\mathbf{r},\mathbf{r}'} \frac{e^2}{|\mathbf{r}-\mathbf{r}'|}\left[n(\mathbf{r})n(\mathbf{r}') - n(\mathbf{r})\delta^d(\mathbf{r}-\mathbf{r}')\right], && (189)\\ &= \int_{\mathbf{r}} \psi_\sigma^\dagger \frac{-\hbar^2\nabla^2}{2m}\psi_\sigma + \frac{1}{2}\int_{\mathbf{r},\mathbf{r}'} \frac{e^2}{|\mathbf{r}-\mathbf{r}'|}\left[\psi_\sigma^\dagger(\mathbf{r})\psi_\sigma(\mathbf{r})\psi_{\sigma'}^\dagger(\mathbf{r}')\psi_{\sigma'}(\mathbf{r}') - \psi_\sigma^\dagger(\mathbf{r})\psi_\sigma(\mathbf{r})\delta^d(\mathbf{r}-\mathbf{r}')\right], && (190)\\ &= \int_{\mathbf{r}} \psi_\sigma^\dagger \frac{-\hbar^2\nabla^2}{2m}\psi_\sigma + \frac{1}{2}\int_{\mathbf{r},\mathbf{r}'} \frac{e^2}{|\mathbf{r}-\mathbf{r}'|}\psi_\sigma^\dagger(\mathbf{r})\psi_{\sigma'}^\dagger(\mathbf{r}')\psi_{\sigma'}(\mathbf{r}')\psi_\sigma(\mathbf{r}), && (191)\end{aligned}$$

where $\psi_\sigma^\dagger(\mathbf{r})$ is the fermionic (anticommuting) field operator that creates an electron at $\mathbf{r}$ and spin σ (sum over repeated spin σ index is implied) and we used units of charge (esu) for which $1/(4\pi\epsilon_0) = 1$. We note that in the many-body form written in terms of number density $n(\mathbf{r}) = \psi_\sigma^\dagger(\mathbf{r})\psi_\sigma(\mathbf{r})$, we took out the formally divergent diagonal contribution, to exclude electron's self interaction, which precisely cancelled in the final form once the fermionic operators are normal-ordered.

It is sometimes convenient to take advantage of translational invariance and work in momentum plane-wave basis, in terms of fermionic operators $c_{\mathbf{k},\sigma}$, defined by

$$\psi_\sigma(\mathbf{r}) = \frac{1}{V^{1/2}}\sum_{\mathbf{k}} c_{\mathbf{k},\sigma} e^{i\mathbf{k}\cdot\mathbf{r}},$$

that annihilate an electron with momentum $\mathbf{k}$ and spin σ. The Hamiltonian in this form is then given by

$$\begin{aligned} H_{el} &= \sum_{\mathbf{k}} \epsilon_k c^\dagger_{\mathbf{k},\sigma} c_{\mathbf{k},\sigma} + \frac{1}{2}\sum_{\mathbf{q}} v_{\mathbf{q}} \tilde{n}(-\mathbf{q})\tilde{n}(\mathbf{q}) - \frac{1}{2} v(0)\tilde{n}(0), & (192)\\ &= \sum_{\mathbf{k}} \epsilon_k c^\dagger_{\mathbf{k},\sigma} c_{\mathbf{k},\sigma} + \frac{1}{2V}\sum_{\mathbf{q},\mathbf{k},\mathbf{k}'} v_{\mathbf{q}} c^\dagger_{\mathbf{k},\sigma} c_{\mathbf{k}-\mathbf{q},\sigma} c^\dagger_{\mathbf{k}',\sigma'} c_{\mathbf{k}'+\mathbf{q},\sigma'} - \frac{1}{2} v(0) \sum_{\mathbf{k}} c^\dagger_{\mathbf{k},\sigma} c_{\mathbf{k},\sigma}\ , & (193)\\ &= \sum_{\mathbf{k}} \epsilon_k c^\dagger_{\mathbf{k},\sigma} c_{\mathbf{k},\sigma} + \frac{1}{2V}\sum_{\mathbf{q},\mathbf{k},\mathbf{k}'} v_{\mathbf{q}} c^\dagger_{\mathbf{k}+\mathbf{q},\sigma} c^\dagger_{\mathbf{k}'-\mathbf{q},\sigma'} c_{\mathbf{k}',\sigma'} c_{\mathbf{k},\sigma}\ , & (194) \end{aligned}$$

where $\tilde{n}(\mathbf{q}$ is the Fourier transform of electron density and $v_{\mathbf{q}}$ is the Fourier transform of the Coulomb potential, in 3d given by $v_{\mathbf{q}} = 4\pi e^2/q^2$.

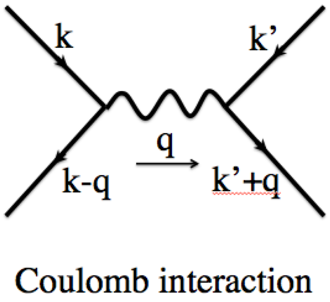

FIG. 15: Feynman diagram representing electron-electron Coulomb interaction (wavy line).

2. Ground-state energy: Hartree-Fock analysis

To calculate the properties of interacting Fermi gas we use perturbation theory in Coulomb interaction about the noninteracting gas limit, analyzed above. Recall that the noninteracting wave function is the Slater determinant forming a Fermi sea

$$|FS\rangle = \prod_{\mathbf{k}<k_F,\sigma} c^\dagger_{\mathbf{k},\sigma}|0\rangle.$$

Standard time-independent perturbation expansion for the ground state energy is given by

$$E_{GS} = \langle FS|H_0|FS\rangle + \langle FS|H_{int}|FS\rangle + \sum_{n\neq FS} \frac{|\langle n|H_{int}|n\rangle|^2}{E_{FS}-E_n} + \ldots, \qquad (195)$$

where $|n\rangle$ are the noninteracting excited states (e.g., electron-hole excitations, etc.) of the Fermi gas, and $E^0_{GS} = E_{FS}$ is the noninteracting Fermi sea ground state energy,

$$E^0_{GS} = \langle FS|H_0|FS\rangle = \langle FS|\sum_{\mathbf{k},\sigma}^{k_F} \epsilon_k c^\dagger_{\mathbf{k},\sigma} c_{\mathbf{k},\sigma}|FS\rangle, \tag{196}$$

$$= \sum_{\mathbf{k},\sigma}^{k_F} \epsilon_k = 2V \int \frac{d^3k}{(2\pi)^3}\frac{\hbar^2k^2}{2m} = N\frac{3}{5}\epsilon_F. \tag{197}$$

To compute the lowest-order corrections due to Coulomb interactions we evaluate

$$\langle FS|H_{int}|FS\rangle = \frac{1}{2V}\sum_{\mathbf{q},\mathbf{k}<k_F,\mathbf{k}'<k_F} v_\mathbf{q}\langle FS|c^\dagger_{\mathbf{k}+\mathbf{q},\sigma}c^\dagger_{\mathbf{k}'-\mathbf{q},\sigma'}c_{\mathbf{k}',\sigma'}c_{\mathbf{k},\sigma}|FS\rangle, \tag{198}$$

$$= \frac{1}{2V}\sum_{\mathbf{q},\mathbf{k}<k_F,\mathbf{k}'<k_F} v_\mathbf{q}\left[\overline{c^\dagger_{\mathbf{k}+\mathbf{q},\sigma}c_{\mathbf{k},\sigma}}\;\overline{c^\dagger_{\mathbf{k}'-\mathbf{q},\sigma'}c_{\mathbf{k}',\sigma'}} - \overline{c^\dagger_{\mathbf{k}+\mathbf{q},\sigma}c_{\mathbf{k}',\sigma'}}\;\overline{c^\dagger_{\mathbf{k}'-\mathbf{q},\sigma'}c_{\mathbf{k},\sigma}}\right], \tag{199}$$

$$= \frac{1}{2V}\sum_{\mathbf{q},\mathbf{k}<k_F,\mathbf{k}'<k_F} v_\mathbf{q}\left[\delta_{\mathbf{q},0} - \delta_{\sigma,\sigma'}\delta_{q,\mathbf{k}'-\mathbf{k}}\right], \tag{200}$$

$$= \frac{1}{2V}\sum_{\mathbf{q},\mathbf{k}<k_F,\mathbf{k}'<k_F,\sigma,\sigma'} (v_0 - v_{\mathbf{k}'-\mathbf{k}}\delta_{\sigma,\sigma'}) \equiv E_{direct} + E_{exchange}, \tag{201}$$

where we used Wick's theorem to average the two-particle correlator with the two contractions corresponding to the direct Hartree and exchange Fock contributions, that are illustrated diagrammatically in Fig.(16). Equivalently, above average can also be evaluated directly by computing the overlap between two-hole excitations states $c_{\mathbf{k}',\sigma'}c_{\mathbf{k},\sigma}|FS\rangle$, by commuting the fermionic annihilation operators through the N creation operators of the Fermi-sea state. The two contributions physically correspond to two electrons filling in the two created holes (direct Hartree) and to exchanging which two holes they fill (hence minus sign in the exchange Fock contribution).

We observe that the direct Hartree term

$$E_{direct} = \frac{1}{2V}\sum_{\mathbf{q},\mathbf{k}<k_F,\mathbf{k}'<k_F,\sigma,\sigma'} v_0 = \frac{1}{2V}N^2 v_0 = \frac{1}{2}Nnv_{\mathbf{q}=0} \tag{202}$$

is actually divergent, proportional to $v_{\mathbf{q}=0}$. To make sense of this it is instructive to look back in real space in terms of $\psi(\mathbf{r})$ fields. The Hartree term is then seen to correspond to

$$E_{direct} = \frac{1}{2}\int_{\mathbf{r},\mathbf{r}'}\frac{e^2}{|\mathbf{r}-\mathbf{r}'|}\langle\psi^\dagger_\sigma(\mathbf{r})\psi_\sigma(\mathbf{r})\rangle\langle\psi^\dagger_{\sigma'}(\mathbf{r}')\psi_{\sigma'}(\mathbf{r}')\rangle = \frac{1}{2}\int_{\mathbf{r},\mathbf{r}'}\frac{e^2}{|\mathbf{r}-\mathbf{r}'|}n^2 = \frac{1}{2}Vv_{\mathbf{q}=0}n^2, \tag{203}$$

where n is the average electron density. We note that in addition to electron-electron interaction, electrons also interact with the positive ionic background charge, that, by charge

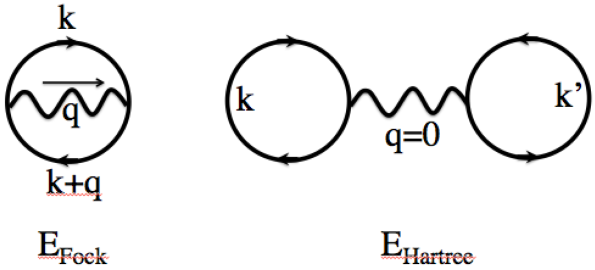

FIG. 16: Feynman diagram representing Hatree-Fock contributions to ground state energy of an electron gas.

neutrality are on average at the same density, n, corresponding to

$$E_{el-ion} = \sum_{i=1}^{N}\int_{\mathbf{r}}\frac{(-e)(en)}{|\mathbf{r}-\mathbf{r}_i|} = -Nnv_{\mathbf{q}=0}. \tag{204}$$

Finally, there is also an electrostatic energy contribution of repulsive ion-ion charge interaction, that contributes

$$E_{ion-ion} = \frac{1}{2}\int_{\mathbf{r},\mathbf{r}'}\frac{(en)^2}{|\mathbf{r}-\mathbf{r}'|} = \frac{1}{2}Nnv_{\mathbf{q}=0}. \tag{205}$$

Combining these with the E_{direct} we find that classical charge interaction gives exactly zero contribution to the electrostatic energy. This exact cancellation is not surprising since overall electron-ion charge system is charge neutral and therefore in the continuum, on average has a vanishing electrostatic energy.

We note that this vanishing of the classical direct Hartree interaction contribution is the property of the *uniform* Fermi gas. In a more interesting situations, where density is nonuniform, e.g., due to a boundary or in the presence of a one-body potential, $U(r)$, the Hatree term gives a nontrivial self-consistently determined density dependent correction to the one-body potential, giving

$$U_{eff}^{Hartree}(r) = U(r) + \int_{\mathbf{r}'} v(\mathbf{r}-\mathbf{r}')\langle\psi^\dagger_\sigma(\mathbf{r}')\psi_\sigma(\mathbf{r}')\rangle.$$

This is a crucial starting ingredient of density functional theory of electron liquid.

However, for a *uniform* electron gas that is our focus here, Coulomb interaction correction to the ground state energy is *negative* and comes only through the exhange interaction, a purely quantum effect,

$$\begin{aligned} E_{exchange} &= -\frac{1}{V}\sum_{\mathbf{k}<k_F,\mathbf{k}'<k_F} v_{\mathbf{k}'-\mathbf{k}}, \qquad (206)\\ &= -V\int_{k_1,k_2<k_F}\frac{d^3k_1}{(2\pi)^3}\frac{d^3k_2}{(2\pi)^3}\frac{4\pi e^2}{|\mathbf{k}_1-\mathbf{k}_2|^2}, \qquad (207)\\ &= \frac{1}{2}\sum_{\mathbf{k},\sigma} n_F(k)\Sigma_{ex}(k), \qquad (208)\\ &= -V\frac{e^2}{4\pi^3}k_F^4 = -N\frac{3e^2}{4\pi}k_F, \qquad (209) \end{aligned}$$

where the final result is obtained after a somewhat technically complicated integration and we defined the exchange self-energy

$$\begin{aligned} \Sigma_{ex}(k) &\equiv -\int\frac{d^3k'}{(2\pi)^3}\frac{4\pi e^2}{|\mathbf{k}-\mathbf{k}'|^2}n_F(k'), \qquad (210)\\ &= -\frac{e^2}{\pi}\int_0^{k_F}dk'k'^2\int_{-1}^{1}\frac{d\mu}{k^2+k'^2-2kk'\mu}, \qquad (211)\\ &= -\frac{e^2}{\pi k}\int_0^{k_F}dk'k'\ln\left|\frac{k+k'}{k-k'}\right|, \qquad (212)\\ &= -\frac{e^2k_F}{\pi}\left(1+\frac{1-x^2}{2x}\ln\left|\frac{1+x}{1-x}\right|\right), \qquad (213) \end{aligned}$$

with $x\equiv k/k_F$, that corrects the free quadratic dispersion relation to be $\epsilon_k^R = \frac{\hbar^2k^2}{2m}+\Sigma_{ex}(k)$, thereby modifying the electron's effective mass.

Combining this with the noninteracting Fermi gas energy, we obtain

$$\begin{aligned} E_{GS} &= N\left[\frac{3}{5}\epsilon_F - \frac{3e^2}{4\pi}k_F\right], \qquad (214)\\ &= N\left[\frac{3}{5}\left(\frac{9\pi}{4}\right)^{2/3}\frac{1}{r_s^2} - \frac{3}{2}\left(\frac{3}{2\pi}\right)^{2/3}\frac{1}{r_s}\right], \qquad (215)\\ &= N\left[\frac{2.21}{r_s^2}-\frac{0.916}{r_s}\right]\left(\frac{e^2}{2a_0}\right), \qquad (216) \end{aligned}$$

where we expressed the result in terms of the characteristic Rydberg energy $E_{Ry} = e^2/(2a_0) = 13.6$ eV and in terms of the key r_s-parameter, defined by

$$r_s = r_0/a_0,$$

which measures electron separation r_0 ($\frac{4}{3}\pi r_0^3 \equiv 1/n$) in terms of Bohr radius $a_0 = 0.51\text{Å}$. Given that electron density n (or equivalently k_F^3) are the only available density scales, the form of the Coulomb contribution e^2/r to the ground-state energy is dictated by dimensional analysis.

There is a lot of physics contained in the above simple result. The attractive interaction is purely quantum statistical consequence of the Pauli principle, that leads to nontrivial statistical correlations in two-electron distribution function. It suppresses the probability of finding an electron with a particular spin (say $\sigma =\uparrow$) $g_\uparrow(\mathbf{r}) = g_{\uparrow\downarrow}(\mathbf{r}) + g_{\uparrow\uparrow}(\mathbf{r})$ from its asymptotic value of 1 (at large r) down to 1/2, because Pauli principle requires $g_{\uparrow\uparrow}(\mathbf{r} \rightarrow 0) = 0$ as it strictly excludes electrons with the same spin from common location. Such correlation exposes the positive ionic background to which the electron is attracted, leading to lowering of the electrostatic energy, a purely quantum-mechanical statistical effect.

Another important observation is that this exchange Fock contribution is only present for spin aligned electrons (for electrons with opposite spins there is no Pauli principle and thus no exchange contribution). Thus, it is only the energy of electrons with aligned spins that is lowered by the Coulomb exchange interaction.

3. *Wigner crystal and quantum melting*

We observe that above expansion of the ground-state energy is controlled by smallness of the Coulomb interaction, which, curiously, corresponds to high density equivalent to large k_F, small electron separation, $r_s \ll 1$. As we can see from E_{GS}, (216), the interaction-to-kinetic energy ratio grows as r_s, leading to breakdown of above small r_s expansion. In fact for conventional metals r_s not small, roughly $3.26(\mathrm{L}i) \leq r_s \leq 5(\mathrm{C}s)$. We thus expect the interaction to dominate at large r_s, small densities, and to lead to quantum crystallization of the electron liquid into electron Wigner crystal, as illustrated in the schematic phase diagram in Fig.(17).

This crystallization at low densities is a purely quantum-mechanical effect, as classically we intuitively expect interaction to instead dominate at large densities (small r_s) and to lead crystallization with increased pressure. The reason for this qualitative distinction is that classically, the interaction that increases with density is to be compared to thermal energy that at fixed temperature is density independent (or just weakly density dependent). In contrast, quantum mechanically, while interaction energy does still increase with increasing density as $1/r_s \sim n^{1/3}$, the kinetic energy $p_F^2/2m \sim 1/r_s^2 \sim n^{2/3}$ increase faster due to

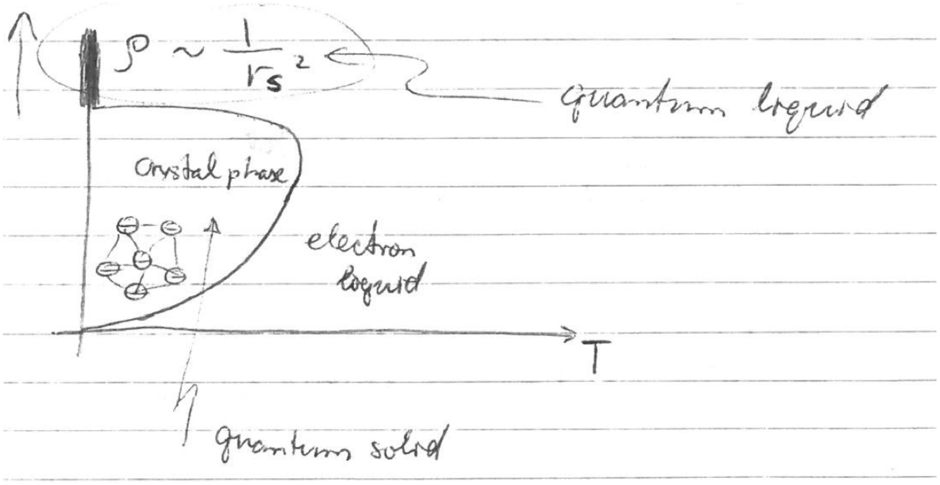

FIG. 17: Density-temperature phase diagram for an electron liquid, showing *quantum* crystallization at low density ρ (large r_s) at low T, where interactions dominate and classical melting at high T, where thermal energy and entropy dominate.

the Heisenberg uncertainty principle (electrons at high density have their position better defined which leads to higher fluctuations in their momentum and therefore kinetic energy) and thus dominates at large density. Thus, Wigner and other quantum crystals actually quantum melt upon squeezing, as is clear from Fig.(17). A two-dimensional Wigner crystal appears for electrons on surface of He4 and also in GaAs heterostructures, where one can create 2d electron liquid, a model system that is also instrumental for a realization of the quantum Hall liquids.

C. Stoner ferromagnetism

In previous sections we have seen the Pauli paramagnetic and Landau diamagnetic responses in the non-interacting Fermi gas. We now examine spin-magnetism in a repulsively interacting Fermi gas. To this end we study the ground-state energy of a short-range interacting electron gas, modeled by a Hamiltonian

$$H_{el} = \int_{\mathbf{r}} \left[\psi_\sigma^\dagger \frac{-\hbar^2\nabla^2}{2m}\psi_\sigma + \frac{1}{2} g\, \psi_\sigma^\dagger(\mathbf{r})\psi_\sigma(\mathbf{r})\psi_{\sigma'}^\dagger(\mathbf{r})\psi_{\sigma'}(\mathbf{r}) \right], \quad (217)$$

$$= \int_{\mathbf{r}} \left[\psi_\sigma^\dagger \frac{-\hbar^2\nabla^2}{2m}\psi_\sigma + \frac{1}{2} g n(\mathbf{r})^2 \right], \quad (218)$$

where for simplicity we have focussed on the zero-range interaction (cutoff at microscopic scale smaller than any other scale in the problem), characterized by a pseudo-potential coupling $g = \frac{4\pi\hbar^2}{m} a_s$, proportional to the s-wave scattering length a_s. We need to compute the ground state energy $E_{GS}(n_\uparrow, n_\downarrow)$ as a function of average spin up and down densities

$$n_\uparrow = \frac{1}{2}(n-m), \quad n_\downarrow = \frac{1}{2}(n+m),$$

respectively, where n and m are the average total density and average magnetization (density difference between the spin up and down electrons).

We next observe that (aside from some short-scale terms) by Pauli principle $n_\sigma^2 = 0$, so the interaction energy can be written as proportional to $n_\uparrow n_\downarrow = \frac{1}{4}(n^2 - m^2)$.

The kinetic energy is straightforwardly evaluated in the FS state. We first recall that for a noninteracting Fermi gas, each spin specie's energy density is given by

$$\mathcal{E}_{GS}^\sigma = \frac{3}{5} n_\sigma \epsilon_{F,\sigma} = \frac{3}{5}\frac{(6\pi^2)^{2/3}\hbar^2}{2m} n_\sigma^{5/3}.$$

For the sum of spin up and down species this is nothing but the expression that led to Pauli paramagnetism, as can be seen by expanding above form to quadratic order in m. Putting this together inside $\mathcal{E}_{GS}$, we find

$$\begin{aligned}
\mathcal{E}_{GS}[m] &= \frac{3}{5}\frac{(6\pi^2)^{2/3}\hbar^2}{2m}\left(n_\uparrow^{5/3} + n_\downarrow^{5/3}\right) + g n_\uparrow n_\downarrow, && (219)\\
&= \frac{3}{10} n\epsilon_F \left[(1-m/n)^{5/3} + (1+m/n)^{5/3}\right] + \frac{1}{4} g n^2 (1 - m^2/n^2), && (220)\\
&= \frac{3}{5} n\epsilon_F + \frac{1}{2}\underbrace{\left(\frac{2\epsilon_F}{3n}\right)}_{1/\chi_{Pauli}} m^2 + \frac{1}{81}\frac{\epsilon_F}{n^3} m^4 + \ldots + \frac{1}{4} g(n^2 - m^2), && (221)\\
&= \frac{3}{5} n\epsilon_F \left[1 + \frac{5}{9}\left(1 - \frac{3gn}{4\epsilon_F}\right)(m/n)^2 + \frac{5}{243}(m/n)^4 + \ldots\right] && (222)
\end{aligned}$$

For small g the energy clearly increases with $|m|$ due to increase in kinetic energy with magnetization m (imbalance m/n). In contrast the s-wave interaction energy is an inverted parabola in m. Thus, as is clear from plots of the $\mathcal{E}_{GS}[m]$ vs m in Fig.(18), the system exhibits an itinerate quantum PM - FM phase transition at a critical value of

$$g_c = \frac{4}{3}\epsilon_F/n,$$

or equivalently, at a critical value of dimensionless ratio of interaction to kinetic Fermi energy, characterized by

$$k_F a_s^c = \pi/2.$$

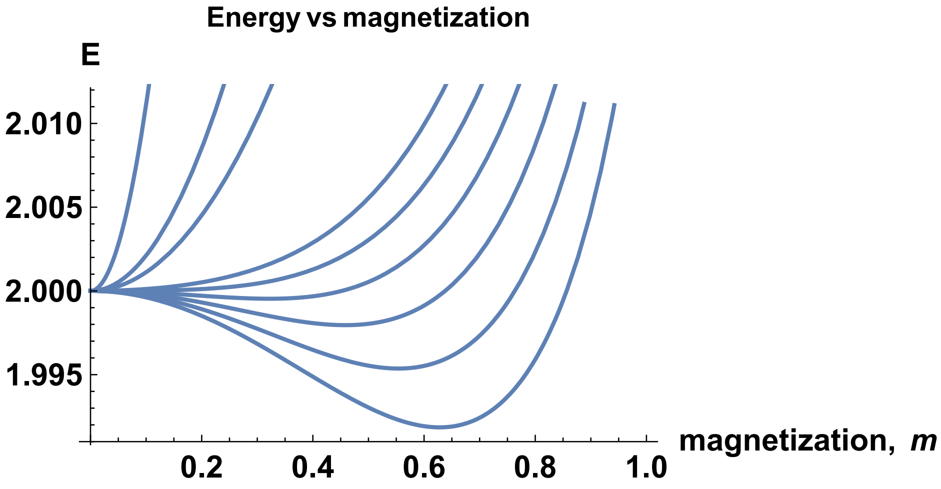

FIG. 18: Energy density of a repulsively interacting Fermi gas as a function of magnetization, illustrating a quantum PM-FM phase transition.

The physics behind this spontaneous magnetic ordering is quite clear. For large repulsive interaction the system can lower its energy by polarizing, i.e., converting into a single spin species of fermions, that, by Pauli principle do not interact via the short s-wave interaction. This interaction-driven tendency to form a FM state is resisted by the kinetic energy that clearly increases with m. For sufficiently strong repulsive interaction and/or large magnetization m and shallow dispersion, a magnetization m *spontaneously* develops for $g > g_c$ through this continuous quantum second order phase transition in the ground state. This spontaneous itinerate FM is referred as Stoner ferromagnetism.

D. Linear screening and density response function

In analysis of an interacting Fermi gas, above, we used a “bare” (in vacuum) Coulomb interation. However, in condensed states, the system (e.g., electrons and ions) can respond to an imposed charge, screening it through induced polarization. Concomitant with this, the interaction between charges (e.g., electrons) is similarly screened by other electrons and ions. Here we study this important physics and as we will see in metals the long-range Coulomb interaction is screened to a Yukawa short-range type. In dielectrics, where there are no free, conducting charges, Coulomb interaction is simply reduced but remains long range.

1. Linear screening

The general theory of electromagnetic screening of course starts with Maxwell equations and involves independent analysis of transverse and longitudinal (to wavevector $\mathbf{k}$) components of $\mathbf{E}$ and $\mathbf{B}$ fields. The former controls the propagation of electromagnetic waves through condensed matter (e.g., the speed of light $c_m(\mathbf{q},\omega) = c/\sqrt{\epsilon_T(\mathbf{q},\omega)}$ in matter), while the latter determines screening of interactions and response to charged impurities, the subject that is our focus here.

Electrical screening is controlled by Gauss's law in matter,

$$\boldsymbol{\nabla}\cdot\mathbf{D} = 4\pi\rho_{ext},$$

where the displacement field is related to the electric field $\mathbf{E}$ and matter polarization $\mathbf{P}$ in the standard way, $\mathbf{D} = \mathbf{E} + 4\pi\mathbf{P}$. Using this inside Gauss's law together with

$$\mathbf{E} = -\boldsymbol{\nabla}V,\ \rho_{ind} = -\boldsymbol{\nabla}\cdot\mathbf{P},\ \rho = -e\delta n,$$

we obtain

$$-\nabla^2 V = 4\pi(\rho_{ext} + \rho_{ind}).$$

For weak screening we can express the induced charge density in terms of the scalar potential, by using a linear relation between induced electron number density δn and the *total* electrical potential energy $(-e)V$, namely

$$\begin{aligned} \rho_{ind}(\mathbf{q},\omega) &= e^2\chi_{sc}(\mathbf{q},\omega)V(\mathbf{q},\omega), && (223)\\ &= e^2\chi(\mathbf{q},\omega)V_{ext}(\mathbf{q},\omega), && (224)\end{aligned}$$

with χ_{sc} the "screened" density response function, related to compressibility $\chi_{sc}(0,0) = \frac{\partial n}{\partial\mu}$ and χ a distinct but related (see below) density response function to *external* electrical potential.

With this, we thus find

$$V(\mathbf{q},\omega) = \frac{4\pi\rho_{ext}(\mathbf{q},\omega)}{\epsilon(\mathbf{q},\omega)}, \qquad (225)$$

where the longitudinal dielectric "constant" is given by

$$\begin{aligned} \epsilon_L(\mathbf{q},\omega) &\equiv \frac{V_{ext}(\mathbf{q},\omega)}{V(\mathbf{q},\omega)}, && (226)\\ &= 1 - \frac{4\pi e^2}{q^2}\chi_{sc}(\mathbf{q},\omega) = \left(1 + \frac{4\pi e^2}{q^2}\chi(\mathbf{q},\omega)\right)^{-1}, && (227)\end{aligned}$$

with the susceptibilities relation

$$\chi(\mathbf{q},\omega) = \frac{\chi_{sc}(\mathbf{q},\omega)}{1 - v_{\mathbf{q}}\chi_{sc}(\mathbf{q},\omega)}, \tag{228}$$

where $v_{\mathbf{q}} = 4\pi e^2/q^2$ is the unscreened Coulomb interaction. For dielectric materials we then obtain the dielectric susceptibility, defined as $\chi_{diel} = -e^2 \lim_{q\to 0} \chi_{sc}(\mathbf{q},0)/q^2$ and the dielectric constant $\epsilon(0,0) = 1 + 4\pi\chi_{diel}$. From its definition we also note that zeros of $\epsilon_L(\mathbf{q},\omega)$ give natural modes of excitations of longitudinal field without an external field, an observation that we will return to later.

From the above definition of $\epsilon_L(\mathbf{q},\omega)$, we also deduce that the effective screened Coulomb interaction, $v_{eff}(\mathbf{q},\omega) = \frac{v_{\mathbf{q}}}{\epsilon_L(\mathbf{q},\omega)}$ is given by

$$v_{eff}(\mathbf{q},\omega) = \frac{v_{\mathbf{q}}}{1 - v_{\mathbf{q}}\chi_{sc}(\mathbf{q},\omega)}, \tag{229}$$

$$= \frac{4\pi e^2/q^2}{1 - \frac{4\pi e^2}{q^2}\chi_{sc}(\mathbf{q},\omega)}, \tag{230}$$

a result that we will rederive shortly using field-theoretic methods.

Utilizing the conductivity relation between induced current density and electric field and charge continuity,

$$\mathbf{J}_{ind}(\mathbf{q},\omega) = \sigma(\mathbf{q},\omega)\mathbf{E}(\mathbf{q},\omega), \quad -i\omega\rho_{ind}(\mathbf{q},\omega) + i\mathbf{q}\cdot\mathbf{J}_{ind}(\mathbf{q},\omega) = 0,$$

we find

$$\epsilon_L(\mathbf{q},\omega) = 1 - \frac{4\pi}{i\omega}\sigma_L(\mathbf{q},\omega). \tag{231}$$

Thus, once density response and/or conductivity are known, dielectric and metallic response can be obtained from above results. We thus now turn to computation of the density response function $\chi_{sc}(\mathbf{q},\omega)$.

2. Density response function

Above screening results can be equivalently obtained using a field theoretic many-body analysis, e.g., through the grassmann coherent-state path-integral for the partition function,

$$\begin{aligned} Z &= Tr\left(e^{-\beta H}\right) = \int \mathcal{D}\overline{\psi}\mathcal{D}\psi e^{-S[\overline{\psi},\psi]}, && (232)\\ &= \int \mathcal{D}\overline{\psi}\mathcal{D}\psi e^{-\int_\tau\left[\int_{\mathbf{r}}\overline{\psi}\hat{G}_0^{-1}\psi+\frac{1}{2}\int_{\mathbf{r},\mathbf{r}'}n(\mathbf{r},\tau)v(\mathbf{r}-\mathbf{r}')n(\mathbf{r}',\tau)\right]}, && (233)\\ &= \int \mathcal{D}\overline{\psi}\mathcal{D}\psi\mathcal{D}\phi e^{-\int_\tau\left[\int_{\mathbf{r}}\overline{\psi}\hat{G}_0^{-1}\psi-\frac{1}{2}\int_{\mathbf{q}}\phi(-\mathbf{q},\tau)v_{\mathbf{q}}^{-1}\phi(\mathbf{q},\tau)+i\int_{\mathbf{q}}\phi(-\mathbf{q},\tau)\overline{\psi}\psi(\mathbf{q},\tau)\right]}, && (234)\\ &= \int \mathcal{D}\overline{\psi}\mathcal{D}\psi\mathcal{D}\phi e^{\frac{1}{2}\int_{\tau,\mathbf{q}}\phi(-\mathbf{q},\tau)v_{\mathbf{q}}^{-1}\phi(\mathbf{q},\tau)-\delta S_{eff}[\phi]}, && (235)\\ & && (236)\end{aligned}$$

where $\hat{G}_0^{-1} = \partial_\tau + \hat{\varepsilon}$ is the inverse of the noninteracting fermionic propagator derived earlier, we used the Hubbard-Stratanovic (HS) transformation (inverse Gaussian integral) to decouple the electron Coulomb interaction (with kernel $v_{\mathbf{q}} = 4\pi e^2/q^2$) by introducing the HS fluctuating scalar potential field ϕ and formally integrated over the resulting quadratic fermionic action to obtain the correction to the effective action,

$$e^{-\delta S_{eff}[\phi]} \equiv \int \mathcal{D}\overline{\psi}\mathcal{D}\psi e^{-\int\left[\overline{\psi}\hat{G}_0^{-1}\psi+\phi\overline{\psi}\psi\right]}. \qquad (237)$$

The effective action

$$S_{eff}[\phi] = \sum_n \frac{1}{n!}\int \Gamma^{(n)}\phi^n,$$

is a power-series in ϕ, with the coefficients $\Gamma^{(n)}$ the so-called 1PIs, i.e., diagrams that cannot be separated into parts by cutting the Coulomb interaction line. The quadratic term $\Gamma^{(2)} = -\chi_{sc}$ illustrated diagrammatically Fig.(19) is of particular interest to us as it determines linear screening, screened density response function χ_{sc}. The associated unscreened density response function χ is the geometric series expansion of (228) in terms of such screened polarization bubbles, diagrammatically illustrated in Fig.(20).

To lowest order the screened response function $\chi_{sc} \approx \chi_0$ is given by the first term in Fig.(19), an approximation that is referred to as the Random Phase Approximation (RPA). By Wick's theorem this electron-hole polarization bubble is given by the convolution of two

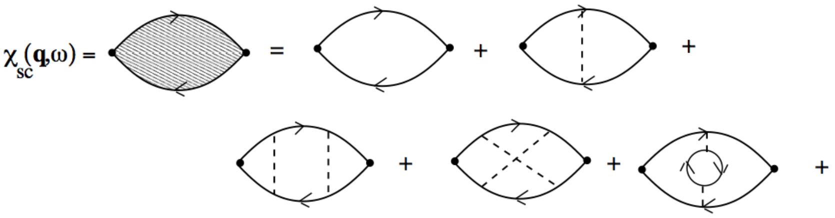

FIG. 19: 1-PI $\Gamma^{(2)}(\mathbf{q},\omega)$ corresponding to the imaginary time density-density correlation function, that for real frequencies gives the screened density response function $\chi_{sc}(\mathbf{q},\omega)$[6].

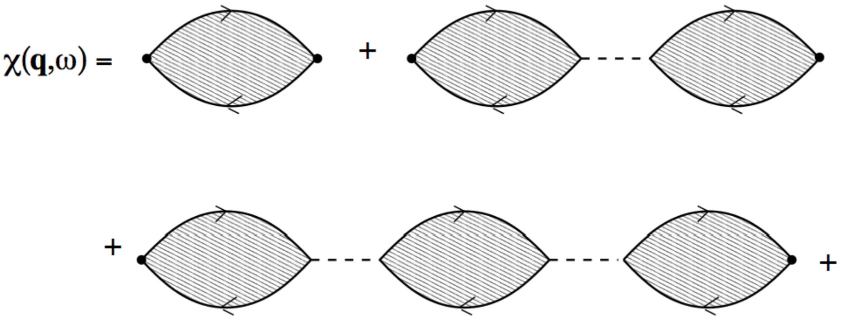

FIG. 20: Diagrammatic expansion of the unscreened density response function $\chi(\mathbf{q},\omega)$ in terms of the screened density response function $\chi_{sc}(\mathbf{q},\omega)$, giving (228)[6].

free fermionic Greens functions

$$
\begin{aligned}
\chi_0(\mathbf{k},\omega_n) &= -\langle\overline{\psi}\psi\overline{\psi}'\psi'\rangle|_{\omega_n,\mathbf{k}}, && (238)\\
&= \langle\overline{\psi}\psi'\rangle\langle\overline{\psi}'\psi\rangle|_{\omega_n,\mathbf{k}}, && (239)\\
&= \int_{\tau,\mathbf{r}} G(\tau,\mathbf{r})G(-\tau,-\mathbf{r})e^{i\omega_n\tau-i\mathbf{k}\cdot\mathbf{r}}, && (240)\\
&= \int_{\nu,\mathbf{q}} G(\nu,\mathbf{q})G(\nu-\omega_n,\mathbf{q}-\mathbf{k}), && (241)\\
&= \int_{\nu,\mathbf{q}} \frac{1}{(i\nu-\varepsilon_{\mathbf{q}})(i(\nu-\omega_n)-\varepsilon_{\mathbf{q}-\mathbf{k}})}, && (242)\\
&= \frac{2\pi i}{2\pi i}\int_{\mathbf{q}}\left[\frac{\theta(\varepsilon_{\mathbf{q}})\theta(-\varepsilon_{\mathbf{q}-\mathbf{k}})}{i\omega_n+\varepsilon_{\mathbf{q}-\mathbf{k}}-\varepsilon_{\mathbf{q}}}+\frac{\theta(-\varepsilon_{\mathbf{q}})\theta(\varepsilon_{\mathbf{q}-\mathbf{k}})}{-i\omega_n+\varepsilon_{\mathbf{q}}-\varepsilon_{\mathbf{q}-\mathbf{k}}}\right], && (243)\\
&= -\int_{\mathbf{q}}\frac{\theta(-\varepsilon_{\mathbf{q}})[1-\theta(-\varepsilon_{\mathbf{q}-\mathbf{k}})]-[1-\theta(-\varepsilon_{\mathbf{q}})]\theta(-\varepsilon_{\mathbf{q}-\mathbf{k}})}{i\omega_n+\varepsilon_{\mathbf{q}-\mathbf{k}}-\varepsilon_{\mathbf{q}}}, && (244)\\
&= -\int_{\mathbf{q}}\frac{\theta(-\varepsilon_{\mathbf{q}})-\theta(-\varepsilon_{\mathbf{q}-\mathbf{k}})}{i\omega_n+\varepsilon_{\mathbf{q}-\mathbf{k}}-\varepsilon_{\mathbf{q}}}, && (245)\\
&= -\int\frac{d^d\mathbf{q}}{(2\pi)^d}\frac{n_F(\varepsilon_{\mathbf{q}})-n_F(\varepsilon_{\mathbf{q}-\mathbf{k}})}{i\omega_n+\varepsilon_{\mathbf{q}-\mathbf{k}}-\varepsilon_{\mathbf{q}}}, && (246)
\end{aligned}
$$

where the theta-functions encode that terms appear only when poles are of particular sign and therefore reside on the correct side of the real axis, and in the last line we generalize to finite T in an obvious way. After analytical continuation to real frequencies $i\omega_n\to\omega+i0^+$, $\chi_{sc}(\mathbf{k},\omega_n)$ encodes the screened density response function

$$\chi_{sc}(\mathbf{k},\omega)=-i\int_{-\infty}^{\infty}dte^{i\omega t}\theta(t)\langle[n_k(t),n_{-k}(0)]\rangle,$$

to an external scalar potential, in the uniform limit a response to the chemical potential, namely the compressibility. In the second line, above, we exchanged fermionic fields to apply Wick's contraction, thereby picking up an additional minus sign.

$\chi_0(\mathbf{k},\omega)$ can now be straightforwardly evaluated at $T=0$. In 3d, to do the $\mathbf{q}$ integral, we analytically continue to real frequencies, shift the variables of integration and then choose z-axis to be along $\mathbf{k}$ and perform the integral in Cartesian coordinates, obtaining

$$
\begin{aligned}
\chi_0(\mathbf{k},\omega) &= -\int_{-q_F}^{q_F}dq_z\int\frac{d^2\mathbf{q}_\perp}{(2\pi)^3}\left[\frac{1}{\omega-q_zk/m+k^2/2m+i0^+}-\frac{1}{\omega-q_zk/m-k^2/2m+i0^+}\right], && (247)\\
&= -\int_{-q_F}^{q_F}dq_z\frac{\pi(q_F^2-q_z^2)}{(2\pi)^3}\left[\frac{1}{\omega-q_zk/m+k^2/2m+i0^+}-\frac{1}{\omega-q_zk/m-k^2/2m+i0^+}\right], && (248)\\
&= -\frac{q_Fm}{4\pi^2}-\frac{1}{8\pi^2}\left(\frac{m}{k}\right)^3\left[\left(\frac{k^2q_F^2}{m^2}-(\omega+k^2/2m)^2\right)\ln\left(\frac{\omega+k^2/2m+kq_F/m+i0^+}{\omega+k^2/2m-kq_F/m+i0^+}\right)\right.\\
&\quad\left.+\left(\frac{k^2q_F^2}{m^2}-(\omega-k^2/2m)^2\right)\ln\left(\frac{\omega-k^2/2m-kq_F/m+i0^+}{\omega-k^2/2m+kq_F/m+i0^+}\right)\right] && (249)
\end{aligned}
$$

The density susceptibility, $\chi_{sc}(\mathbf{k},\omega)$ also gives the dielectric function via

$$\epsilon_L(\mathbf{k},\omega) = 1 - \frac{4\pi e^2}{k^2}\chi_{sc}(\mathbf{k},\omega), \tag{250}$$

that in the static $\omega \to 0$ and $\mathbf{k} \to 0$ limits gives $\chi_0(0,0) = -\frac{q_F m}{4\pi^2} \equiv -\frac{k_{TF}^2}{4\pi e^2}$, with $k_{TF}^2 = \frac{3\pi e^2 n_0}{\epsilon_F} = 4\pi e^2 g(\epsilon_F)$, $n_0 = q_F^3/(6\pi^2)$, which leads to Thomas-Fermi screening, $V(k) = 4\pi e^2/(\varepsilon(k)k^2) = e^2/(k^2 + k_{TF}^2)$. In real space the latter leads to short-ranged potential of Yukawa type, $V(r) \sim e^{-k_{TF}r}/r$.

At finite frequency and $k \to 0$, this function also gives $\epsilon(\omega,0) = 1 - \omega_p^2/\omega^2$, with the plasmon frequency given by $\omega_p^2 = 4\pi n e^2/m \sim \sqrt{e^2 q_F \epsilon_F} \sim \epsilon_F\sqrt{r_s}$. Note that the imaginary parts of χ_0, involve argument of the logarithmic function and give either 0 or π given the infinitesimal $i0^+$.

The behavior of imaginary part of $\chi_0(\mathbf{k},\omega)$ depends strongly on the regime of $\omega, \mathbf{k}$, determined by whether the frequency falls into the 2-particle continuum, bounded by two curves: $\omega < k^2/2m \pm kq_F$, technically distinguished by the phase of the argument of the logarithms being 0 or π:

- $k > 2q_F$
  - * $0 < \omega < k^2/2m - kq_F/m$:
    $Im(\chi_0) = 0$
  - * $k^2/2m - kq_F/m < \omega < k^2/2m + kq_F/m$:
    $Im(\chi_0) = \frac{m}{8\pi k}\left[q_F^2 - \frac{m^2}{k^2}(\omega - k^2/2m)^2\right]$
  - * $\omega > k^2/2m + kq_F/m$:
    $Im(\chi_0) = 0$
- $k < 2q_F$
  - * $0 < \omega < kq_F/m - k^2/2m$
    $Im(\chi_0) = \frac{m^2}{4\pi}\frac{\omega}{k}$
  - * $kq_F/m - k^2/2m < \omega < k^2/2m + kq_F/m$:
    $Im(\chi_0) = \frac{m}{8\pi k}\left[q_F^2 - \frac{m^2}{k^2}(\omega - k^2/2m)^2\right]$
  - * $\omega > k^2/2m + kq_F/m$:
    $Im(\chi_0) = 0$

We note that despite a qualitative change in form between first two regimes for $k < 2q_F$, $\chi_0''(\mathbf{k},\omega)$ is indeed continuous across the dotted curve (see Fig.(21)).

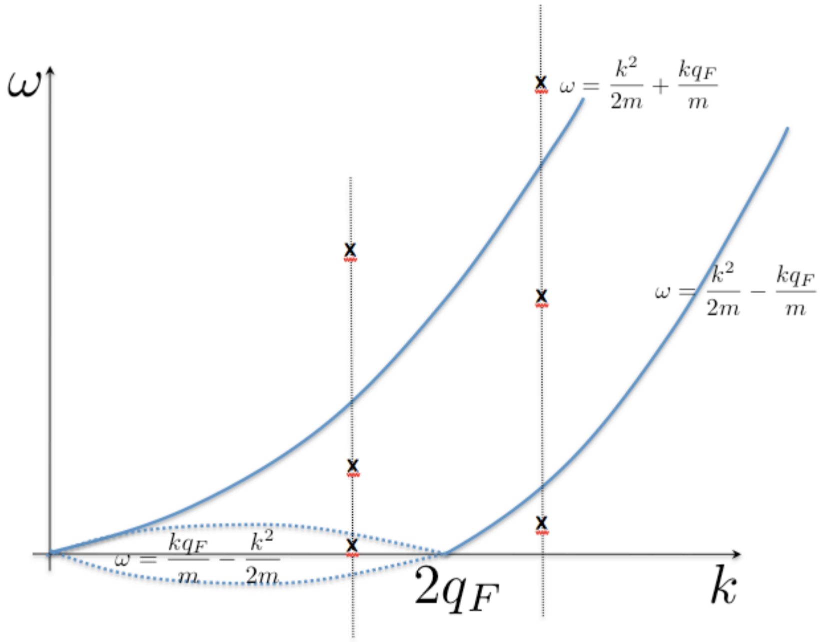

FIG. 21: Two-particle continuum and corresponding regions of distinct behavior of $\chi_0(\mathbf{k},\omega)$ marked by ×'s. As discussed in detail in the text, the imaginary part of the density response function, $\chi_0''(\mathbf{k},\omega)$ is nonzero only between the full lines. There is a change in the behavior of $\chi_0''(\mathbf{k},\omega)$ across the dotted line.

In the static limit $\omega = 0$, we find the standard result (Lindhardt dielectric function)

$$\begin{aligned}
\chi_0(\mathbf{k},0) &= -\frac{q_F m}{4\pi^2} - \frac{1}{4\pi^2}\left(\frac{m}{k}\right)^3\left[\left(\frac{k^2q_F^2}{m^2} - (k^2/2m)^2\right)\ln\left|\frac{k^2/2m + kq_F/m}{k^2/2m - kq_F/m}\right|\right], && (251)\\
&= -\frac{1}{8\pi^2}\frac{q_F^3}{\varepsilon_F}\left[1 + \frac{1}{2x}(1-x^2)\ln\left|\frac{1+x}{1-x}\right|\right], && (252)
\end{aligned}$$

where $x = k/2k_F$, proportional to the density of states n/ϵ_F. For small k ($x \to 0$) the function is well-behaved, going as $-\frac{k_{TF}^2}{4\pi e^2}(1 - x^2/3 + O(x^4))$, at $x = 1$ exhibits an infinite slope singularity in the $\log|1-x|$, i.e., the so-called Kohn anomaly at $k = 2q_F$, associated with the existence of a sharp Fermi surface. As a result of Kohn anomaly the screened potential $V_{sc}(r) \sim \cos(2k_F r)/r^3$ exhibits Friedel oscillations and decays as a power-law (rather than the exponential Thomas-Fermi result) for $r \to \infty$. The function vanishes at large k.

It is constructive to also evaluate the screened response function $\chi_0(\mathbf{k}, \omega)$ in various limits directly from its basic form, (246).

limit $\omega \ll v_F k$:

In this limit, we can neglect the frequency and at $T = 0$ and small k find

$$\chi_0(\mathbf{k}, 0) \; = \; \int \frac{d^d\mathbf{q}}{(2\pi)^d} \frac{n_F(\varepsilon_{\mathbf{q}}) - n_F(\varepsilon_{\mathbf{q}-\mathbf{k}})}{\varepsilon_{\mathbf{q}} - \varepsilon_{\mathbf{q}-\mathbf{k}}} = \int_0^\infty d\epsilon g(\epsilon) \frac{\partial n_F(\epsilon)}{\partial \epsilon} = -g(\epsilon_F), \qquad (253)$$

where we used the density of states and the fact that in the low T limit $\frac{\partial n_F(\epsilon)}{\partial \epsilon} = -\delta(\epsilon - \epsilon_F)$. Using this inside (250), we find

$$\epsilon(\mathbf{k}, 0) = 1 + \frac{k_{TF}^2}{k^2},$$

where

$$k_{TF}^2 = 4\pi e^2 g(\epsilon_F) = \frac{6\pi n e^2}{\epsilon_F}.$$

limit $\omega \gg v_F k$:

Starting again with (246), analytically continuing to real frequencies, and in the second term changing variables $\mathbf{q} \to -(\mathbf{q} - \mathbf{k})$, the terms combine into a form that simplifies in the above limit of small ω and low T:

$$\chi_0(\mathbf{k}, \omega) \; = \; \int \frac{d^d\mathbf{q}}{(2\pi)^d} n_F(\varepsilon_{\mathbf{q}}) \left[\frac{1}{\omega_n + i0 + \varepsilon_{\mathbf{q}} - \varepsilon_{\mathbf{q}-\mathbf{k}}} - \frac{1}{\omega_n + i0 + \varepsilon_{\mathbf{q}-\mathbf{k}} - \varepsilon_{\mathbf{q}}} \right], \qquad (254)$$

$$= \; 2 \int \frac{d^d\mathbf{q}}{(2\pi)^d} n_F(\varepsilon_{\mathbf{q}}) \frac{\varepsilon_{\mathbf{q}-\mathbf{k}} - \varepsilon_{\mathbf{q}}}{(\omega_n + i0)^2 - (\varepsilon_{\mathbf{q}-\mathbf{k}} - \varepsilon_{\mathbf{q}})^2}, \qquad (255)$$

$$\approx \; \frac{1}{m\omega^2} \int \frac{d^d\mathbf{q}}{(2\pi)^d} n_F(\varepsilon_{\mathbf{q}})(k^2 - 2\mathbf{k} \cdot \mathbf{q}) = \frac{nk^2}{m\omega^2}. \qquad (256)$$

This then gives the dielectric function

$$\epsilon_F(0, \omega) = 1 - \frac{\omega_p^2}{\omega^2},$$

where the plasma frequency is given by

$$\omega_p^2 = \frac{4\pi n e^2}{m}.$$

Indeed $\epsilon_L(\mathbf{k}, \omega) = 0$ gives the dispersion of longitudinal excitations of the electron liquid. In this $\mathbf{k} \to 0$ limit this gives the longitudinal charge density oscillations, namely the plasmon $\omega = \omega_p + O(q^2)$ found earlier through hydrodynamic description by looking at collective charge density oscillations of an electron liquid. Since these expressions also emerges from more general hydrodynamics, and are supported by a "sum-rule", as emphasized by Pines and Nozieres, above plasmon expressions are exact for $\mathbf{k} = 0$.

Using the expression (231) for dielectric function in terms of conductivity, we find that this real ϵ_L corresponds to a conductivity of a perfect conductor, given by $\sigma(0, \omega) = \frac{ne^2}{m}\left(\pi\delta(\omega) + \frac{i}{\omega}\right)$. This unphysical RPA result will be modified once the physics of a finite electron scattering rate $1/\tau$ is included.

More generally, $\epsilon_L(\mathbf{k}, \omega) = 0$ gives the full dispersion of excitations of an interacting electron gas, which in terms of the density response function $\chi_{sc}(\mathbf{k}, \omega)$ within RPA gives

$$1 = \frac{4\pi e^2}{k^2}\chi_0(\mathbf{k}, \omega), \tag{257}$$

$$= \frac{4\pi e^2}{k^2} V^{-1} \sum_{\mathbf{q}} \frac{n_F(\varepsilon_{\mathbf{q}-\mathbf{k}}) - n_F(\varepsilon_{\mathbf{q}})}{\omega + \varepsilon_{\mathbf{q}-\mathbf{k}} - \varepsilon_{\mathbf{q}} + i0}. \tag{258}$$

This equation can be solved graphically It leads to the electron-hole two-particle continuum

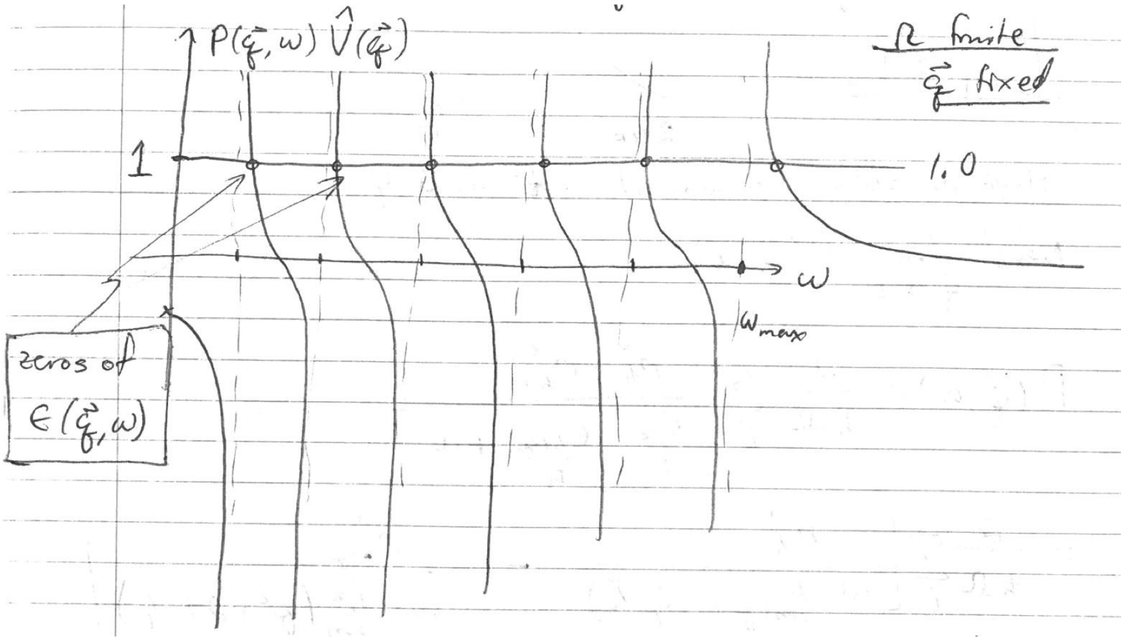

FIG. 22: Graphical solution of $\epsilon_L(\mathbf{k}, \omega) = 0$, that in the thermodynamic $L \to \infty$ limit leads to the two-particle electron-hole continuum and the plasmon mode illustrated in Fig.(7) and Fig.(21).

as well as the plasmon mode of charge density collective excitations, as illustrated Fig.(7) and Fig.(21).

3. Thomas-Fermi screening

Recall that the screening effects are captured by the Poisson equation in a medium for the electrostatic potential,

$$-\nabla^2 V = 4\pi(-e)(n_{ext} + n_{ind}),$$

where the key relation is the linear response $n_{ind}(\mathbf{q},\omega) = -\chi_{sc}(\mathbf{q},\omega)eV(\mathbf{q},\omega)$, valid for weak V. A more direct approach to static ($\omega = 0$) Thomas-Fermi screening (1928) can be obtained by a local density approximation that deduces χ_{sc} from a linear local relation between induced number density $n_{ind}(\mathbf{r})$ and local chemical potential $\mu(\mathbf{r}) = -eV(\mathbf{r})$, namely the local compressibility.

To this end we recall the relation between density and chemical potential in a uniform (for simplicity spinless) system,

$$n(\epsilon_F) = \frac{k_F^3}{6\pi^2} = \frac{(2m\epsilon_F/\hbar^2)^{3/2}}{6\pi^2}.$$

Examining the single particle Hamiltonian $H = p^2/2m - \mu + (-eV(\mathbf{r}))$, it is clear that $eV(r)$ enters on the same footing as the chemical potential. For a potential $V(r)$ varying smoothly on the scale $1/k_F$, it is valid to employ the local density approximation akin to WKB method, and in the presence of a potential $V(\mathbf{r})$ replace chemical potential $\mu = \epsilon_F$ by its local form

$$\epsilon_{TF}(\mathbf{r}) = \epsilon_F + eV(\mathbf{r}),$$

which leads to

$$\begin{aligned} n(\mathbf{r}) &= \frac{(2m\epsilon_{TF}(\mathbf{r})/\hbar^2)^{3/2}}{6\pi^2} = \frac{(2m/\hbar^2)^{3/2}(\epsilon_F + eV(\mathbf{r}))^{3/2}}{6\pi^2}, && (259) \\ &\approx n + \left(\frac{3}{2}\frac{n}{\epsilon_F}\right) eV(\mathbf{r}) = n + \frac{\partial n}{\partial \epsilon_F} eV(\mathbf{r}). && (260) \\ &\equiv n + n_{ind}(\mathbf{r}), && (261) \end{aligned}$$

Using that compressibility is given by $\chi = -\frac{\partial n}{\partial \epsilon_F} = -\frac{\partial}{\partial \epsilon_F}\int_0^{\epsilon_F} d\epsilon g(\epsilon) = -g(\epsilon_F)$, we find

$$n_{ind}(\mathbf{r}) = -\chi_{TF} eV(\mathbf{r}),$$

where

$$\chi_{TF} = -\frac{3}{2}\frac{n}{\epsilon_F} = -g(\epsilon_F),$$

which agrees with our earlier results of the previous subsections, (253).

IV. ELECTRON-PHONON INTERACTION

Above we have studied interacting electron gas in the jelium model approximation where ions are treated as a uniform positive neutralizing potential. Of course in reality the full many-body problem involves interacting quantum dynamics of both ions and electrons. However, as first noted by Born and Oppenheimer (1927), because electrons' typical velocity ($v_F \sim 10^6$ m/s) is much larger than the sound velocity ($c_s \sim 10^3$ m/s) the slow ions are seen by fast electrons as an instantaneous potential. The corresponding many-body wavefunction of electrons and ions is expected to be well approximated by the Borh-Oppenheimer form

$$\Psi(\{\mathbf{r}_i\}, \{\mathbf{R}_l\}) = \sum_n \Phi_n(\{\mathbf{R}_l\})\psi_n(\{\mathbf{r}_i\}, \{\mathbf{R}_i\}),$$

where $\psi_n(\{\mathbf{r}_i\}, \{\mathbf{R}_i\})$ is the electronic eigenfunction for a specific fixed ionic configuration $\{\mathbf{R}_i\}$. The corresponding amplitude $\Phi_n(\{\mathbf{R}_i\})$ is the ionic eigenfunction the Schrodinger many-body equation with the ion-ion interaction $\frac{1}{2}\sum_{l,l]} U(\mathbf{R}_l - \mathbf{R}_{l'})$ corrected by the eigenvalue $E_n^{el}(\{\mathbf{R}\})$ of the electrons' Schrodinger's equation and the Berry's vector and scalar potentials[11]

$$\mathbf{A}_{nn'}(\{\mathbf{R}_l\}) = \frac{\hbar^2}{M}\langle\phi_n|\boldsymbol{\nabla}_{\mathbf{R}}\phi_{n'}\rangle, \tag{262}$$

$$V_{nn'}(\{\mathbf{R}_l\}) = \frac{\hbar^2}{2M}\langle\phi_n|\nabla^2_{\mathbf{R}}\phi_{n'}\rangle. \tag{263}$$

.

Ignoring the Berry's terms and noting that in this adiabatic approximation the ions are in their ground state form, a crystal lattice, the problem reduces to that of electrons moving in a periodic ionic potential. As we have discussed in earlier lectures and has been studied extensively in Solids-I, this leads to the electronic band structure, a spectrum of band separated by gaps. The result is the well-studied phenomenology of electronic band structure that explains the distinction between metals (odd number of electrons per unit cell with Fermi level in the middle of the band of states) and band insulators (even number of electrons per unit cell with Fermi level in the middle of the gap of states).

To go beyond this simple band structure picture we need to take into account quantized modes of vibrations of ionic crystal, namely the phonons. A lattice distortion

$$\mathbf{u}(\mathbf{r}) = \sum_{\mathbf{q}\alpha} \ell_{\mathbf{q},\alpha} \mathbf{e}_{\mathbf{q},\alpha} e^{i\mathbf{q}\cdot\mathbf{r}} \left(a_{\mathbf{q}\alpha} + a^{\dagger}_{-\mathbf{q}\alpha} \right),$$

(where $\ell_{\mathbf{q},\alpha} = \sqrt{\frac{\hbar}{2MN\omega_{\mathbf{q},\alpha}}}$ is quantum length of the phonon mode $\alpha, \mathbf{q}$ and $\mathbf{e}_{\mathbf{q},\alpha}$ is the corresponding polarization), modifies electrons' single-body potential, that couples to electron density

$$n(\mathbf{r}) = \psi^{\dagger}(\mathbf{r})\psi(\mathbf{r}) = \frac{1}{V} \sum_{\mathbf{k}\mathbf{k}'\sigma} e^{i(\mathbf{k}-\mathbf{k}')\cdot\mathbf{r}} \phi^{*}_{\mathbf{k}'}(\mathbf{r}) \phi_{\mathbf{k}}(\mathbf{r}) c^{\dagger}_{\mathbf{k}'\sigma} c_{\mathbf{k}\sigma}.$$

This leads to the electron-phonon Hamiltonian, $H = H_{el} + H_{ph} + H_{el-ph}$, where

$$H_{el} = \sum_{\mathbf{k}\sigma} \varepsilon_{\mathbf{k}} c^{\dagger}_{\mathbf{k},\sigma} c_{\mathbf{k},\sigma}, \tag{264}$$

$$H_{ph} = \sum_{\mathbf{q}} \hbar\omega_{\mathbf{q},\alpha} a^{\dagger}_{\mathbf{q}\alpha} a_{\mathbf{q}\alpha}, \tag{265}$$

$$H_{el-ph} = \sum_{\mathbf{q},\mathbf{k},\alpha,\sigma} g_{\alpha}(\mathbf{q}) \left(a_{\mathbf{q}\alpha} + a^{\dagger}_{-\mathbf{q}\alpha} \right) c^{\dagger}_{\mathbf{k}+\mathbf{q},\sigma} c_{\mathbf{k},\sigma}, \tag{266}$$

where the coupling $g_{\alpha}(\mathbf{q})$ is determined by the nature of the electron-phonon coupling. There are three types of electron-phonon interactions: (i) deformation potential of longitudinal acoustic or optical phonons, (ii) acoustic phonons in piezoelectric crystals, (iii) polar coupling to optical phonons in ionic crystals. We examine these in more detail in the next three subsections. The existence of electron-phonon interaction is crucial for understanding electron scattering at high temperature, that determines electric and thermal transport, equilibration, sound attenuation, etc. We consider a one-electron zero-phonons state $|\mathbf{k}\rangle = c^{\dagger}_{\mathbf{k},\sigma}|0\rangle$ scattered into a one-electron one-phonons state $|\mathbf{k}-\mathbf{q}, 1_{\mathbf{q},\alpha}\rangle = c^{\dagger}_{\mathbf{k}-\mathbf{q},\sigma} a^{\dagger}_{\mathbf{q},\alpha}|0\rangle$. Its scattering

FIG. 23: Graphical Feynman diagram representation for the electron-phonon interaction vertex and its conjugate.

rate is determined by the Fermi-Golden Rule, given by

$$W_{\mathbf{k}\mathbf{k}'} = \frac{2\pi}{\hbar}|\langle \mathbf{k}-\mathbf{q}, 1_{\mathbf{q},\alpha}|H_{el-ph}|\mathbf{k}\rangle|^2 \delta(\varepsilon_{\mathbf{k}} - \varepsilon_{\mathbf{k}-\mathbf{q}} - \hbar\omega_{\mathbf{q},\alpha})\delta_{\mathbf{k}',\mathbf{k}-\mathbf{q}}.$$

The scattering rate is then given by

$$\begin{aligned}\frac{1}{\tau} &= \frac{2\pi}{\hbar}\sum_{\mathbf{q},\alpha}|\langle \mathbf{k}-\mathbf{q}, 1_{\mathbf{q},\alpha}|H_{el-ph}|\mathbf{k}\rangle|^2 \delta(\varepsilon_{\mathbf{k}} - \varepsilon_{\mathbf{k}-\mathbf{q}} - \hbar\omega_{\mathbf{q},\alpha}) \\ &+ \frac{2\pi}{\hbar}\sum_{\mathbf{q},\alpha}|\langle \mathbf{k}+\mathbf{q}|H_{el-ph}|\mathbf{k}, 1_{\mathbf{q},\alpha}\rangle|^2 \delta(\varepsilon_{\mathbf{k}} - \varepsilon_{\mathbf{k}-\mathbf{q}} + \hbar\omega_{\mathbf{q},\alpha}) \qquad (267)\end{aligned}$$

by summing over final states and including phonon absorption and emission processes. This result can equivalently be obtained from the imaginary part of the energy correction to second order in H_{el-ph}, giving $1/\tau \sim T^3$ at low T and $1/\tau \sim T$ at high T.

Similarly, using second order perturbation theory of the single-phonon state (or equivalently a field-theoretic analysis in e.g., the coherent state formulation), we find that electron-hole bubble corrects phonon dispersion,

$$\hbar\omega_\alpha(\mathbf{q}) = \hbar\omega^0_\alpha(\mathbf{q}) - g^2\sum_{\mathbf{k},\sigma}\frac{n_F(\mathbf{k})(1-n_F(\mathbf{k}+\mathbf{q}_))}{\varepsilon_{\mathbf{k}+\mathbf{q}} - \varepsilon_{\mathbf{k}}}. \qquad (268)$$

This correction is proportional electron density-density correlation function, and exhibits a Kohn anomaly, a suppression at $q = 2k_F$ in the phonon dispersion.

The effects is strongest in 1d (where nesting is perfect) and leads to softenning of the phonon as T is lowered. One can think of this as Bose-condensation of $2k_F$ phonon at T_c, leading to crystal's instability against a distortion at $2k_F$. For an initially half-filled electron band, $2k_F = \pi/a$, this Peierls dimerization distortion doubles the unit cell and opens up a electronic gap at the Fermi surface, thereby lowering the electronic energy at the expense of lattice distortion. Concommittant with this electron liquid develops a $2k_F$ charge density wave (CDW), openning a gap in the electronic spectrum and thereby lowering the electronic energy of the filled states.

A. Deformation-potential phonon coupling

One important form of electron-phonon interaction arises in non-ionic crystals, where the electron charge interacts with the deformation potential induced by phonon lattice distortion

$u(\mathbf{r})$. To see this we consider the microscopic electron-phonon interaction

$$H_{el-ph} = \sum_{i=1}^{N_e} V_{lattice}(\mathbf{r}_i) = \int d^d r \rho(\mathbf{r}) V_{lattice}(\mathbf{r}) = \int d^d r \psi_\sigma^\dagger(\mathbf{r})\psi_\sigma(\mathbf{r}) V_{lattice}(\mathbf{r}),$$

where the lattice ionic potential is given by

$$\begin{aligned} V_{lattice}(\mathbf{r}) &= \sum_n V_{ion}(\mathbf{r}-\mathbf{R}_n-\mathbf{u}_n) \approx \sum_n V_{ion}(\mathbf{r}-\mathbf{R}_n) - \sum_n \mathbf{u}_n \cdot \boldsymbol{\nabla} V_{ion}(\mathbf{r}-\mathbf{R}_n), && (269) \\ &= \sum_n V_{ion}(\mathbf{r}-\mathbf{R}_n) - \frac{i}{N}\sum_{\mathbf{q}} e^{i\mathbf{q}\cdot(\mathbf{r}-\mathbf{R}_n)} \mathbf{u}_{\mathbf{q}} \cdot \mathbf{q} V_{ion}(\mathbf{q}), && (270) \end{aligned}$$

where the first term is the perfect (undistorted) periodic lattice potential that leads to the electronic band structure, and the second term leads to the electron-phonon interaction. Putting this together with decomposition into phonon and electron momentum operators we obtain the deformation potential with the electron-phonon coupling given by

$$g_\alpha(\mathbf{q}) = \ell_{\mathbf{q},\alpha} i\mathbf{q} \cdot \hat{\mathbf{e}}_{\alpha,\mathbf{q}}.$$

We note that this coupling is to longitudinal phonons and vanishes in the long wavelength limit.

B. Piezoelectric phonon coupling

Many materials lacking inversion symmetry generically exhibit a piesoelectric coupling, namely a strain, u_{ij} induces an electric field E_i response and vice versa, summarized by

$$E_k = S_{ijk} u_{ij},$$

where S_{ijk} is the piezoelectric response tensor that depends on the specific crystal structure. This is quite common and important in semiconductors, weaker in III-V family like GaAs, and much stronger in II-VI materials like CdS and ZnO.

Since the strain $u_{ij} = \frac{1}{2}(\partial_i u_j + \partial_j u_i)$ is proportional to the gradient of $\mathbf{u}$ and the electric field $\mathbf{E} = -\boldsymbol{\nabla} V$ is proportional to the gradient of the electrostatic potential V, the latter is proportional to the ionic displacement

$$V(\mathbf{r}) \propto \mathbf{u}(\mathbf{r}),$$

and leads to the piezoelectric crystals' electron-phonon coupling given by

$$g_\alpha(\mathbf{q}) = S_{ijk}\ell_{\mathbf{q},\alpha}\frac{q_i q_k}{q^2}\hat{e}^j_{\alpha\mathbf{q}} \equiv \mathbf{S}\cdot\hat{\mathbf{e}}_{\alpha\mathbf{q}}.$$

We note that in contrast to the deformation potential discussed above, for optical phonon (characterized by a nonvanishing ω_q in $q \to 0$ limit), such piezoelectric coupling remains finite (though highly anisotropic) in the long wavelength limit and couples to both longitudinal (LA) and transverse (TA) acoustic phonons. In the simplest approximation it can be treated as a constant, orientational lattice average of the above coupling.

C. Polar optical phonon coupling

Another important electron-phonon coupling takes place in ionic crystals, where positive and negative ions oscillate out of phase, i.e., corresponds to an optical phonon that couples strongly to electrons through the electric polarization and field $\mathbf{P} = -\mathbf{E}/4\pi \propto \rho_0\mathbf{u}(\mathbf{r})$ that it induces. The induced electrostatic potential $V(\mathbf{r})$ is related to the corresponding to the induced charge density, $\rho = \boldsymbol{\nabla}\cdot\mathbf{P} \propto -\rho_0\boldsymbol{\nabla}\cdot\mathbf{u}$, through the Coulomb's law,

$$V(\mathbf{q}) = \frac{4\pi\rho(\mathbf{q})}{q^2} \propto \frac{4\pi\rho_0 i\mathbf{q}\cdot\mathbf{u}_\mathbf{q}}{q^2},$$

which leads to the leading to the electron-phonon coupling

$$g_\alpha(\mathbf{q}) = \alpha\frac{4\pi\rho_0 i\mathbf{q}\cdot\hat{e}^j_{\alpha\mathbf{q}}\ell_{\mathbf{q}\alpha}}{q^2}.$$

Quite clearly the coupling here is only to *longitudinal* optical phonons, that is much stronger at long wavelengths (scaling as $1/q$, since for optical phonons ω_q is finite at small q) than the deformation potential and piezoelectric couplings.

V. STRONGLY INTERACTING ELECTRON LIQUID

A. Hubbard and t-J models

B. Mott insulators and magnetism

VI. ELECTRICAL TRANSPORT

A. Classical Drude model

B. Boltzmann equation

C. Semiclassical transport

D. Kubo formula

VII. SUPERCONDUCTIVITY

A. History and experimental observations

B. Microscopic BCS theory

C. BCS-BEC crossover in Feshbach resonant Fermi gases

D. Ginzburg-Landau theory

---

[1] L.D. Landau and E.M. Lifshitz, Statistical Physics, Part 2 (Pergamon, Oxford, 1980).

[2] P. Nozieres, Theory of interacting Fermi systems (Be- jamin, New York 1964).

[3] D. Pines and P. Nozieres, The theory of quantum liquids, Vol. 1 Normal Fermi liquids (Bejamin, New York 1966).

[4] G. Baym and C. Pethick, Landau Fermi-liquid theory (Wiley, Ney York 1991).

[5] N. F. Mott, Metal-Insulator Transitions, second edition (Taylor and Francis, London, 1990).

[6] *Fundamentals of the Physics of Solids I*, Electronic Properties, J. Solyom.

[7] *Many-Particle Physics*, G. Mahan.

[8] *Quantum Field Theory of Many-body Systems*, Xiao-Gang Wen.

[9] *Path Integrals*, R. P. Feynman and Hibbs. plore properties of this

[10] S. Sachdev, “Quantum phase transitions” (Cambridge University Press, London, 1999).

[11] Quantum Mechanics, R. Shankar.